Naval Research Laboratory

Washington, DC 20375-5320

NRL/MR/7264--19-9901

NRL UINSAR Field Campaign Report and Data Description

MARK SLETTEN
STEVEN MENK

Image Science and Applications Branch
Remote Sensing Division

ROBERT LIANG

Coastal and Ocean Remote Sensing Branch
Remote Sensing Division

August 20, 2019

REPORT DOCUMENTATION PAGE

Form Approved
OMB No. 0704-0188

1. REPORT DATE *(DD-MM-YYYY)*	**2. REPORT TYPE**	**3. DATES COVERED** *(From - To)*
20-08-2018	NRL Memorandum Report	31-07-2017 - 05-02-2018

4. TITLE AND SUBTITLE

NRL UINSAR Field Campaign Report and Data Description

5a. CONTRACT NUMBER

5b. GRANT NUMBER

5c. PROGRAM ELEMENT NUMBER
62435N

6. AUTHOR(S)

Mark Sletten, Steven Menk, and Robert Liang

5d. PROJECT NUMBER

5e. TASK NUMBER
BE-435-056

5f. WORK UNIT NUMBER
6A54

7. PERFORMING ORGANIZATION NAME(S) AND ADDRESS(ES)

U.S. Naval Research Laboratory
4555 Overlook Avenue, SW
Washington, DC 20375-5320

8. PERFORMING ORGANIZATION REPORT NUMBER

NRL/MR/7264--19-9901

9. SPONSORING / MONITORING AGENCY NAME(S) AND ADDRESS(ES)

10. SPONSOR / MONITOR'S ACRONYM(S)

11. SPONSOR / MONITOR'S REPORT NUMBER(S)

12. DISTRIBUTION / AVAILABILITY STATEMENT

DISTRIBUTION STATEMENT A: Approved for public release; distribution is unlimited.

13. SUPPLEMENTARY NOTES

14. ABSTRACT

This report documents deployments of the NRL UHF Interferometric SAR (UINSAR) in July 2017 and January-February 2018. The UINSAR antenna switching configuration, filename conventions, flight geometry, and flight tracks are documented, along with plots of contemporaneous meteorological and oceanographic measurements collected by NOAA buoys located close to the UINSAR collection sites. It is intended to both support NRL's internal analysis of the extensive, unique UHF SAR database collected during these deployments as well as to facilitate collaborative analysis with outside investigators.

15. SUBJECT TERMS

Synthetic aperture radar UHF
Interferometric SAR

16. SECURITY CLASSIFICATION OF:			**17. LIMITATION OF ABSTRACT**	**18. NUMBER OF PAGES**	**19a. NAME OF RESPONSIBLE PERSON**
					Mark Sletten
a. REPORT	**b. ABSTRACT**	**c. THIS PAGE**	Unclassified Unlimited	44	**19b. TELEPHONE NUMBER** *(include area code)*
Unclassified Unlimited	Unclassified Unlimited	Unclassified Unlimited			202-404-7971

This page intentionally left blank.

CONTENTS

This page intentionally left blank.

NRL UINSAR Field Campaign Report and Data Description

1. Introduction

This report documents deployments of the NRL UHF Interferometric SAR (NRL UINSAR) in July 2017 and January-February 2018. The UINSAR antenna switching configuration, filename conventions, flight geometry, and flight tracks are documented, along with plots of contemporaneous meteorological and oceanographic measurements collected by NOAA buoys located close to the UINSAR collection sites. It is intended to both support NRL's internal analysis of the extensive, unique UHF SAR database collected during these deployments as well as to facilitate collaborative analysis with outside investigators.

The basic objective of these flights was to generate a database to support the development of advanced, UHF SAR-based techniques to measure ocean surface currents. For three decades, along-track interferometric synthetic aperture radar (ATI-SAR) has been under development as a sensor for this application. From the earliest single-beam experiments, through the development of vector, dual-beam systems as well as in recent space-borne implementations, SAR systems operating in the microwave band above 1 GHz have been used [1, 2, 3]. This frequency choice was driven primarily by the desire for high spatial resolution coupled with practical limits on antenna size and along-track spacing. However, the higher microwave band poses a challenge when it comes to extracting the true surface *current* from the ATI-SAR measurement of the surface *velocity.* Due to the influence of transient capillary waves in the microwave band and their modulation by longer ocean waves, it can be difficult to accurately model and then remove the wave-induced component of the measured velocity in order to determine the underlying current.

The UHF band promises to alleviate this problem while also opening up new approaches to surface current measurement. In the UHF band, the fundamental radar scattering centers are longer-lived surface waves with wavelengths on the order of 1 m, as opposed to transient capillaries, thereby simplifying the required scattering model. But in addition, the wide azimuthal beamwidth of a typical UHF SAR supports a second, completely independent approach to current measurement. Through sub-aperture processing of the wide-beam data, a time sequence of wave-like images can be produced that contains information on any underlying currents that may be present. Currents alter the dispersion relation between the wavelength and propagation speed of the surface waves, and the image time-sequence provided by sub-aperture processing promises to provide a means to measure this alteration. This “wave dispersion” approach has been used effectively with *land-based, real-aperture* radars as well as with optical systems to measure both currents as well as bathymetry [4, 5], but attempts to implement it with a SAR though sub-aperture processing have not yet been reported in the literature. These potential UHF SAR advantages are currently under investigation using the unique database collected during the deployments documented in this report.

The primary collection site was the Atlantic Ocean east of Maryland, Virginia, and North Carolina. The particular focus was the north wall of the Gulf Stream in this area, as the sharp change in current over this boundary constitutes a strong, reliable feature with which to test our new current measurement algorithms. Our flight tracks were designed to cover the most likely location of the north wall, based upon an informal analysis of available AVHRR imagery (https://marine.rutgers.edu/cool/sat_data/?product=sst&region=sw06&nothumbs=0). Two NOAA buoys are located in this area, NDBC 44014 and NDBC 44009, and this report includes wind and wave data collected by these in situ sensors around the UINSAR collection times. Data were also collected over the Webster Field Annex to the Patuxent Naval Air Station in St. Inigoes MD, Point Lookout MD, and the nearby Chesapeake Bay. These locations provide land imagery that includes a calibration target (deployed

Manuscript approved August 12, 2019.

at Webster Field) as well as additional spatially varying currents. NDBC station PPTM2 provides wind information for this general area, and NOAA also provides tidal current predictions for the nearby Chesapeake Bay and Potomac River (https://tidesandcurrents.noaa.gov/noaacurrents/Predictions?id=ACT4796_2). Data from these additional stations as well as the tidal predictions are also included in this report.

While the primary objective of these deployments was to generate the data required to investigate new algorithms for surface current measurement, the dataset obviously has wider applicability. UHF SAR provides a means to directly sense longer waves on the ocean surface and to therefore remotely monitor the natural processes and human activities that generate them.

2. Nominal UINSAR Flight Geometry

As shown below in Fig. 1, the UINSAR collected data at altitudes of either 1524 m (5000 ft) or 5182 m (17,000 ft). The antennas were boresited at 30º grazing, producing corresponding slant ranges of either 3048 or 10364 m. Acceptable signal-to-noise ratios are generally found across a swath width of approximately 6000 m at an altitude of 5000 ft and 8700 m when collecting at an altitude of 17,000 ft. The nominal airspeed was 130 m/s (250 kts), although the ground speed often varied significantly from pass to pass due to high winds. The actual average ground speed for each pass is listed later in this report in the Pass Summary for each day.

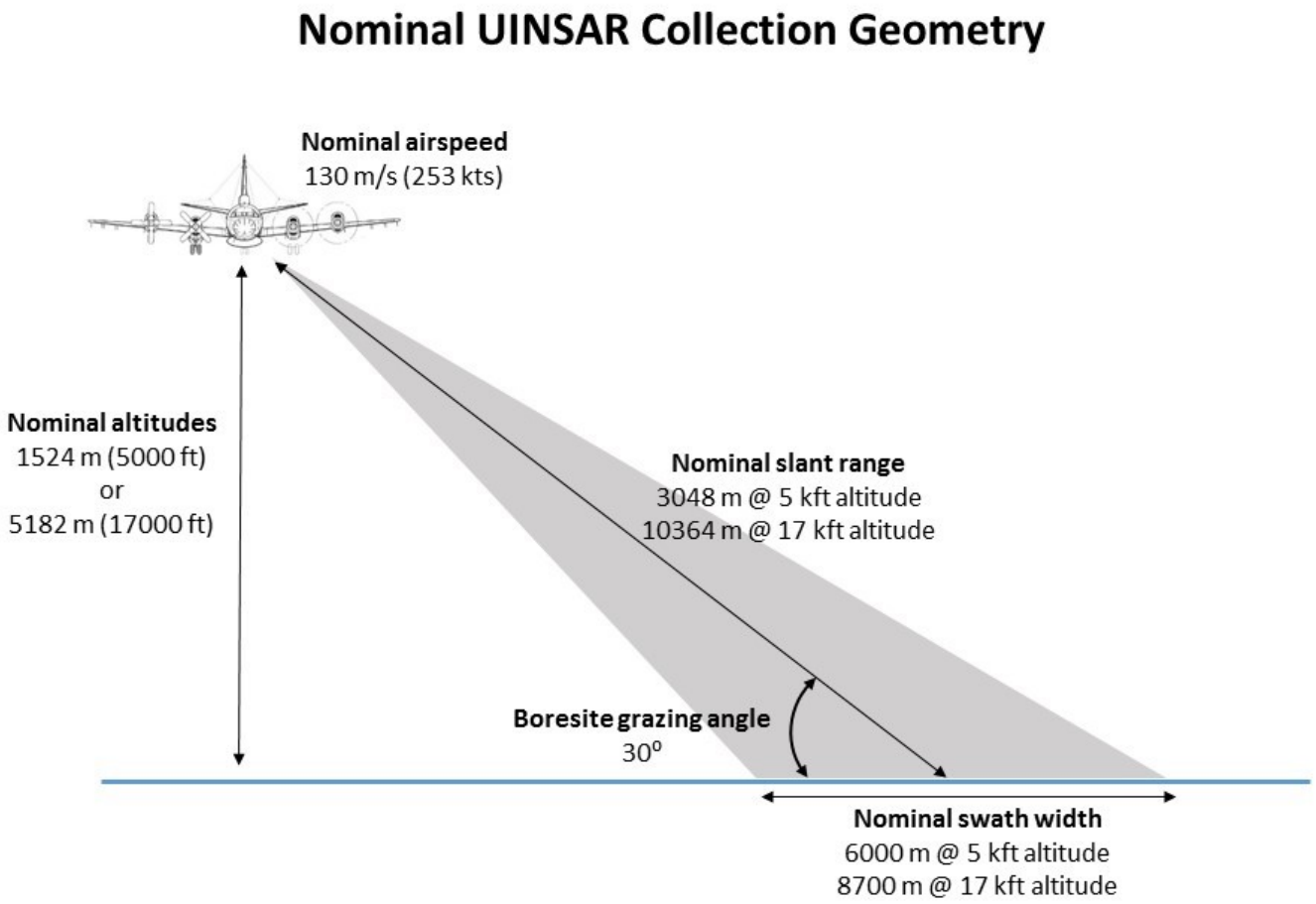

Fig. 1 Nominal UINSAR collection geometry used August 2017 and January-February 2018

3. UINSAR Antenna Configuration and Switching Modes

The NRL UINSAR is a multi-band, multi-phase center system based upon the commercially available KEYW KeyRadar. For the flights described in this report, the system supported 6 simultaneous receive channels and 2 simultaneous transmit channels. Four of the receive channels were devoted to the UHF band while the remaining two supported L-band, and each band used a single transmit channel, switched between either polarization ports on a single antenna or between antennas in different locations on the aircraft. (See below). Due to a combination of spectral management requirements and image formation considerations, each of the four UHF receive channels were partitioned into four simultaneous RF subbands: 230-290 MHz, 290-348 MHz, 352-410 MHz, and 410-450 MHz. For L-band, all data were collected in a single 1000-1400 MHz subband.

As configured for the deployments documented in this report, three antennas were mounted on the NRL P3 aircraft, tail number 570. A single dual-polarized UHF antenna was mounted in the nose radome, while an identical unit plus a dual polarized L-band antenna were mounted in the tail. See Fig. 2. All antennas were boresited at a grazing angle of 30º and all looked to the port side, perpendicular to the long axis of the aircraft.

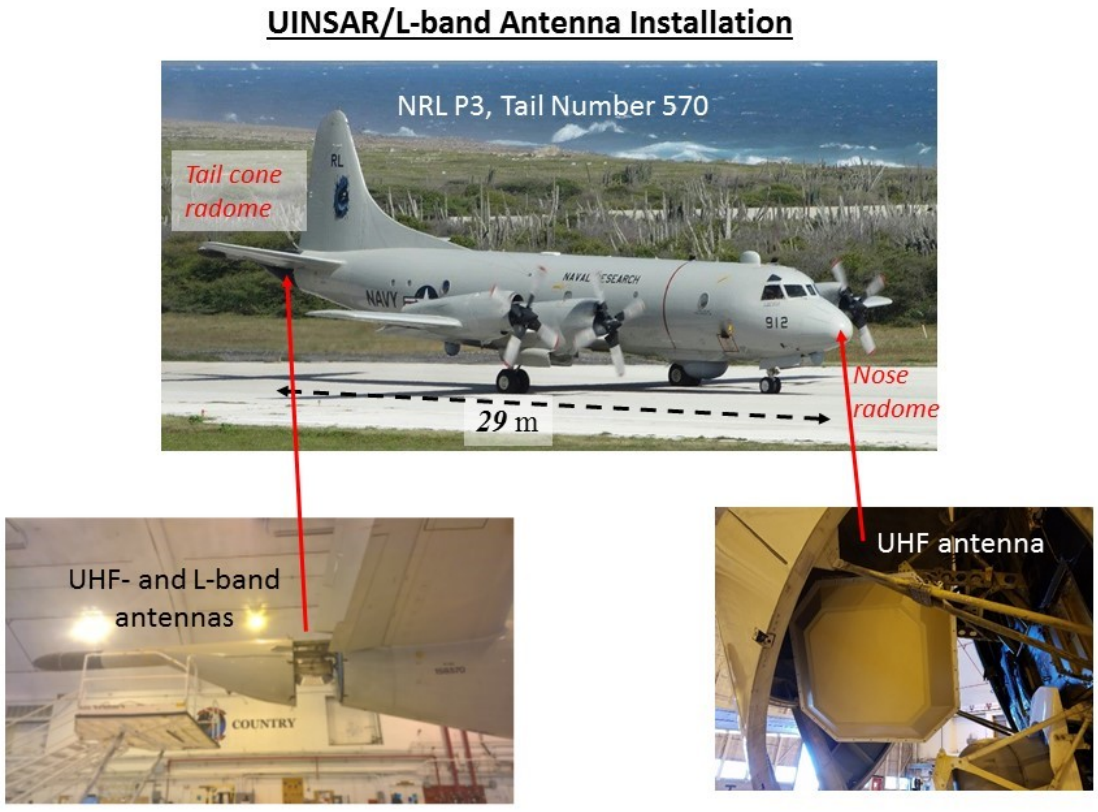

1

Fig. 2 Photographs indicating the locations of the UINSAR antennas onboard the NRL P3 aircraft

UHF SAR data were collected in two different modes with regards to transmit antenna switching. In the "Clutter" mode, only the tail-mounted antenna was used for transmission, and the transmitted polarization was alternated between V and H on a pulse-to-pulse basis. For every pulse, backscatter was received from both the V and H ports of both the nose and tail antennas using the UINSAR's four UHF receive channels. This produced two fully polarimetric phase centers, located midway between the nose and tail and in the tail, separated by 14.5 m. See Fig. 3 below. The Clutter Mode was given its name because the fully polarimetric data it generates provides the best possible characterization of the ocean clutter

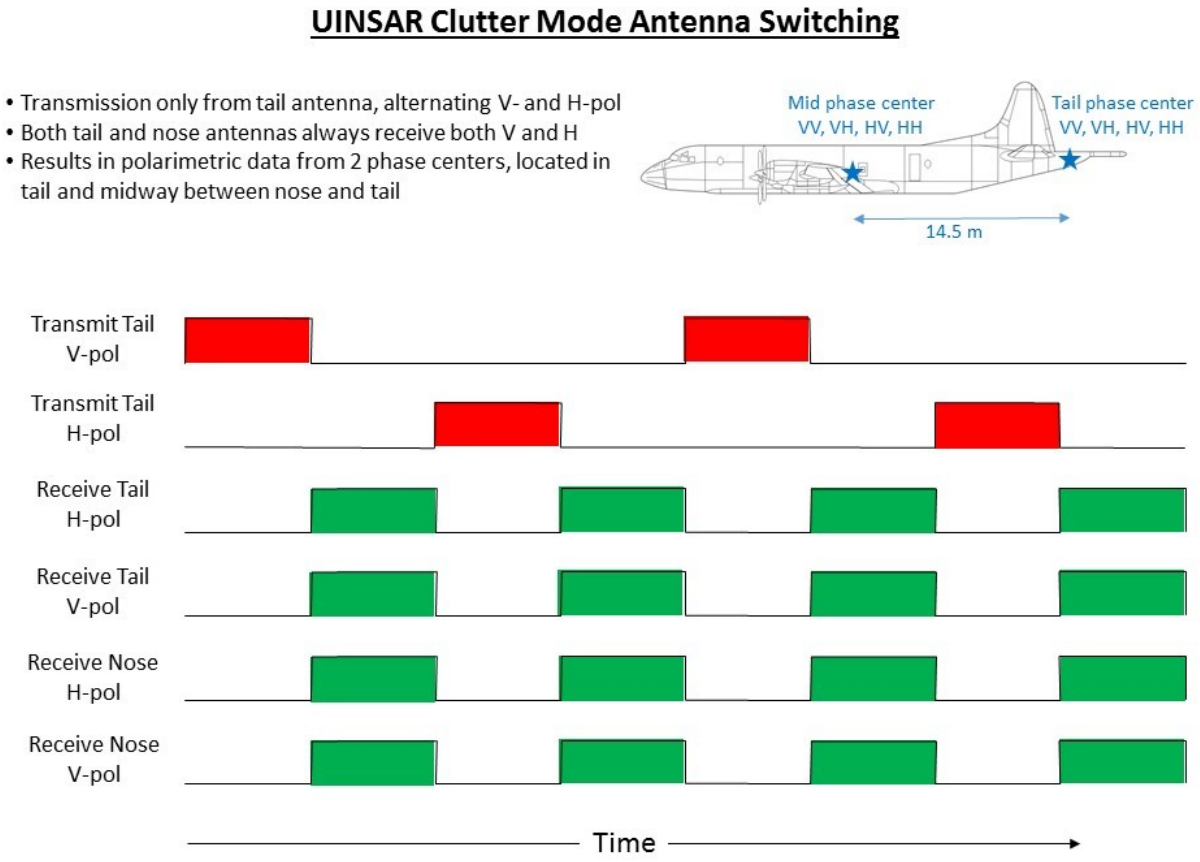

Fig. 3 Description of the antenna switching used in the Clutter mode

The second UINSAR switching mode was named “Ping Pong”. In this mode, transmission alternated between the nose and tail antennas on a pulse-to-pulse basis, but only V-pol was transmitted. As for the Clutter mode, backscatter was always received from both the V and H ports of both the tail and nose antennas. This produced three phase centers, located in the nose, midway between the nose and tail, and in the tail, with each providing VV and VH data. See Fig. 4 below. This mode gets its name from the ping-pong-like alternation between the nose and tail.

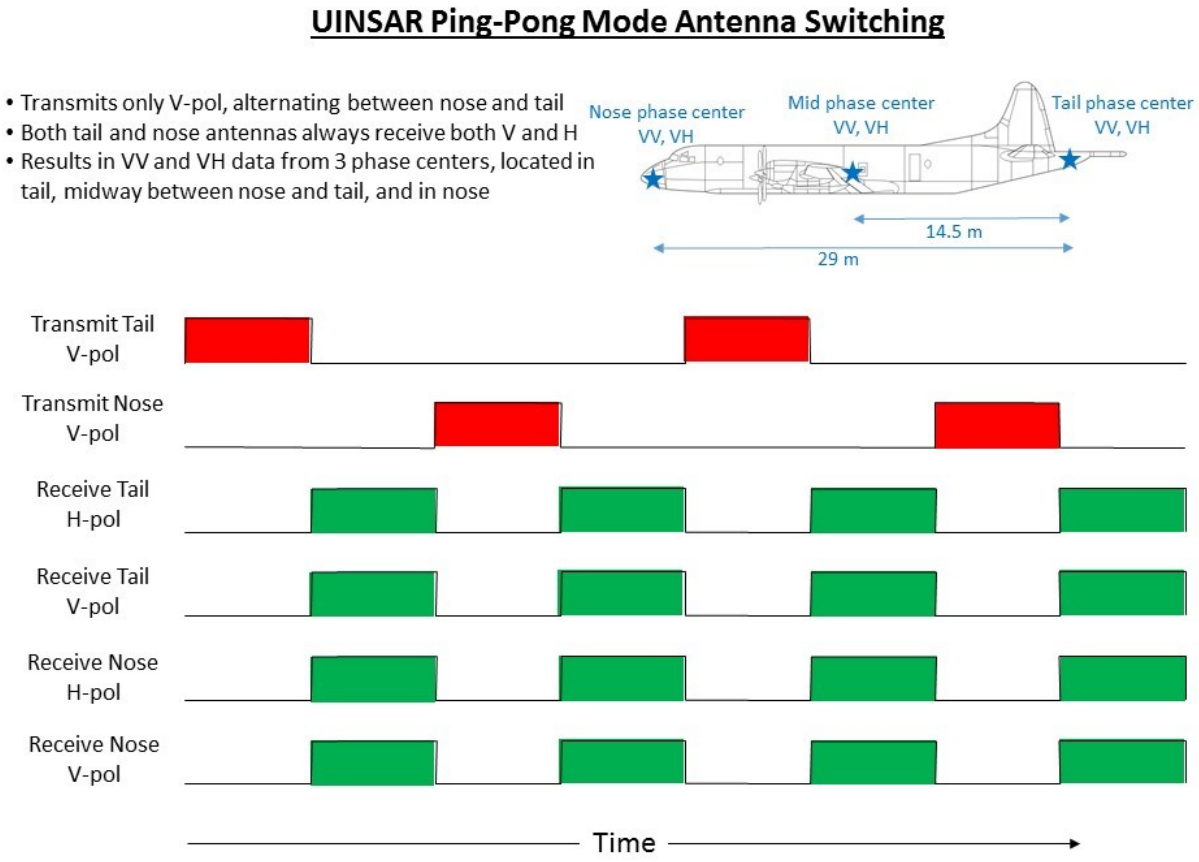

Fig. 4 Description of the antenna switching used in the Ping Pong mode

Regardless of whether the UINSAR was operated in Clutter or Ping Pong mode, L-band data were always collected from the tail-mounted L-band antenna in a standard polarimetric mode. See Fig. 5 below.

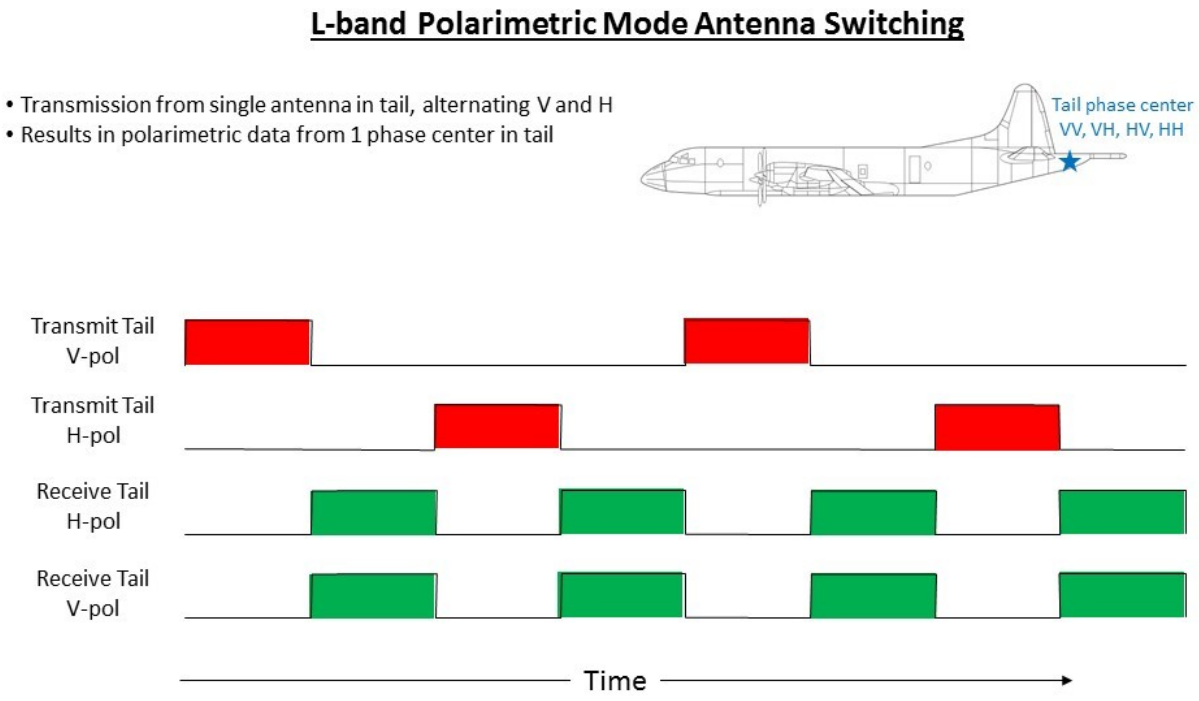

Fig. 5 Description of the antenna switching used for the polarimetric L-band channel

4. Image Filename Conventions

Fig. 6 shows an example filename generated by the software used to process the raw UINSAR data into SAR images. The Date and GMT Time stamps are taken directly from the timestamp of the aircraft pass (listed in the Pass Summary for each flight, below) corresponding to the raw data file. Along with knowledge of the switching mode (Clutter or Ping Pong), combinations of the "A/D converter ID", "Frequency Band", and "Antenna and polarization" fields identify the image's phase center, polarization, and frequency band. These three fields together are referred to as the "filename core". The correspondence between the filename core and the phase center, polarization, and frequency band are given in Tables 1, 2, and 3 for the four UHF subbands. Tables 1 and 2 apply to Ping Pong mode while Table 3 applies to Clutter mode. In Ping Pong mode, the phase center and polarization for a given image file can actually be determined from the "Antenna and Polarization" field alone, as descibed by Table 2. In Clutter mode, the situation is more complex and care must be taken to also select the image whose filename contains the "A/D converter ID" that corresponds to the desired phase center and polarization. As indicated in Fig. 6, the occurrence of P1, P2, and the letter S in the "Antenna and Polarization" field can be used to determine which antennas were transmitting and receiving. The particular sample filename In Fig. 6 corresponds to a 230-290 MHz image collected on July 31, 2017 at 20:40:09 GMT, using Clutter mode and the VV phase center in the tail. In this particular case, the switching mode can be determined from the filename itself, since this particular filename core only occurs for Clutter mode. But there are other cores that appear in both Tables 1 and 3, and thus in general the switching mode cannot be determined from the filename alone.

For the L-band images, the filenames are much simpler, since only a single phase center and a single RF subband are used. The filename core is of the form "X_YYY_F_1000-1400_LP$_T$P$_R$_", where P$_T$ specifies the transmit polarization (V or H) and PR specifies the receive polarization (V or H).

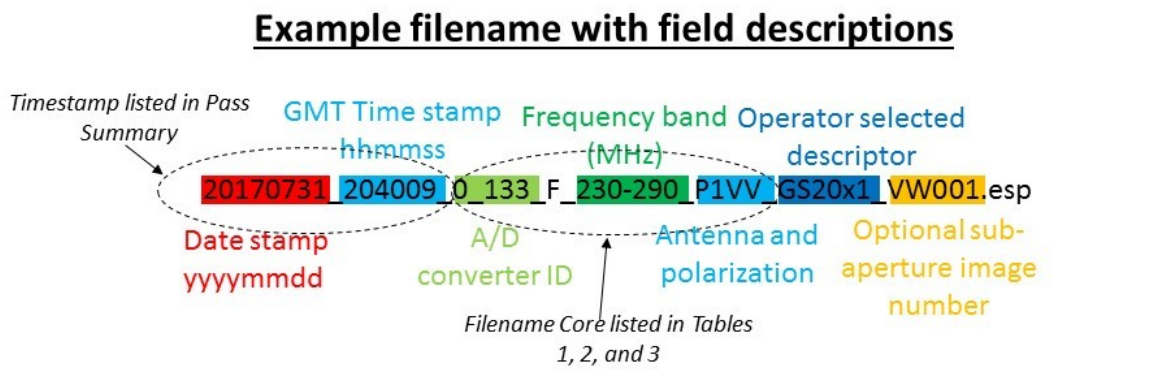

Fig. 6 Description of the fields that make up the UINSAR image filenames

UNISAR Ping-Pong Mode Filenames Cores		
230-290 MHz		
Phase Center	**VV filename core**	**VH filename core**
Tail	0_129_F_230-290_P1VV	0_1_F_230-290_P1VH
Mid ($T_{tail}R_{nose}$)	2_129_F_230-290_P2SV	2_1_F_230-290_P2SH
Mid ($T_{nose}R_{tail}$)	0_133_F_230-290_P1SV	0_5_F_230-290_P1SH
Nose	2_133_F_230-290_P2VV	2_5_F_230-290_P2VH
290-348 MHz		
Phase Center	**VV filename core**	**VH filename core**
Tail	0_130_F_290-348_P1VV	0_2_F_290-348_P1VH
Mid ($T_{tail}R_{nose}$)	2_130_F_290-348_P2SV	2_2_F_290-348_P2SH
Mid ($T_{nose}R_{tail}$)	0_134_F_290-348_P1SV	0_6_F_290-348_P1SH
Nose	2_134_F_290-348_P2VV	2_6_F_290-348_P2VH
352-410 MHz		
Phase Center	**VV filename core**	**VH filename core**
Tail	0_131_F_352-410_P1VV	0_3_F_352-410_P1VH
Mid ($T_{tail}R_{nose}$)	2_131_F_352-410_P2SV	2_3_F_352-410_P2SH
Mid ($T_{nose}R_{tail}$)	0_135_F_352-410_P1SV	0_7_F_352-410_P1SH
Nose	2_135_F_352-410_P2VV	2_7_F_352-410_P2VH
410-450 MHz		
Phase Center	**VV filename core**	**VH filename core**
Tail	0_132_F_410-450_P1VV	0_4_F_410-450_P1VH
Mid ($T_{tail}R_{nose}$)	2_132_F_410-450_P2SV	2_4_F_410-450_P2SH
Mid ($T_{nose}R_{tail}$)	0_136_F_410-450_P1SV	0_8_F_410-450_P1SH
Nose	2_136_F_410-450_P2VV	2_8_F_410-450_P2VH

UINSAR Ping Pong Mode Filename Cores Quick Guide		
Phase center location	**VV filename core**	**VH filename core**
Tail	P1VV	P1VH
Mid ($T_{tail}R_{nose}$)	P2SV	P2SH
Mid ($T_{nose}R_{tail}$)	P1SV	P1SH
Nose	P2VV	P2VH

Table 1 (Upper) Correspondence between the filename cores and the phase center, polarization, and RF band in Ping Pong mode

Table 2 (Lower) Condensed version of Table 1. In Ping Pong mode, the phase center and polarization corresponding to a given image file can be determined by the Antenna and Polarization field alone.

UNISAR Clutter Mode Filename Cores				
230-290 MHz				
Phase Center	**VV filename core**	**VH filename core**	**HV filename core**	**HH filename core**
Tail	0_133_F_230-290_P1VV	0_5_F_230-290_P1VH	0_129_F_230-290_P1HV	0_1_F_230-290_P1HH
Mid ($T_{tail}R_{nose}$)	2_133_F_230-290_P2SV	2_5_F_230-290_P2SH	2_129_F_230-290_P2SV	2_1_F_230-290_P2SH
290-348 MHz				
Phase Center	**VV filename core**	**VH filename core**	**HV filename core**	**HH filename core**
Tail	0_134_F_290-348_P1VV	0_6_F_290-348_P1VH	0_130_F_290-348_P1HV	0_2_F_290-348_P1HH
Mid ($T_{tail}R_{nose}$)	2_134_F_290-348_P2SV	2_6_F_290-348_P2SH	2_130_F_290-348_P2SV	2_2_F_290-348_P2SH
352-410 MHz				
Phase Center	**VV filename core**	**VH filename core**	**HV filename core**	**HH filename core**
Tail	0_135_F_352-410_P1VV	0_7_F_352-410_P1VH	0_131_F_352-410_P1HV	0_3_F_352-410_P1HH
Mid ($T_{tail}R_{nose}$)	2_135_F_352-410_P2SV	2_7_F_352-410_P2SH	2_131_F_352-410_P2SV	2_3_F_352-410_P2SH
410-450 MHz				
Phase Center	**VV filename core**	**VH filename core**	**HV filename core**	**HH filename core**
Tail	0_136_F_410-450_P1VV	0_8_F_410-450_P1VH	0_132_F_410-450_P1HV	0_4_F_410-450_P1HH
Mid ($T_{tail}R_{nose}$)	2_136_F_410-450_P2SV	2_8_F_410-450_P2SH	2_132_F_410-450_P2SV	2_4_F_410-450_P2SH

Table 3 Correspondence between the filename cores and the phase center, polarization, and RF band in Clutter mode

5. Flight Descriptions

This section contains information on each flight conducted in 2017 and 2018. For each flight, a GoogleEarth image is presented that indicates the regions that were covered, along with the Pass Summary where the time stamp, a descriptive passname, the switching mode, and the aircraft heading and average ground speed are listed for each pass. For flights over the Atlantic, plots of the significant wave height, wave direction, wind speed, and wind direction, as measured by nearby NOAA NDBC buoys, are also shown. For all flights, plots of the predicted tidal currents in the Chesapeake Bay near Pt. Lookout are included, as are plots of the wind speed and direction as measured by NDBC Station PPTM2 on Piney Point, MD. These data are included to support analysis and interpretation of imagery collected during each flight over the nearby Webster Field Annex to the Patuxent Naval Air Station (referred to hereafter as "Webster Field" or just "Webster").

5.1 July 31, 2017

On July 31, 2017, data were collected over Webster Field, Point Lookout, and the Chesapeake Bay using both linear and circular passes. Linear pass data for all cardinal look directions were also collected over NOAA NDBC buoy 44014 east of Virginia Beach and over the Gulf Stream east of the Outer Banks of NC. Linear pass data were also collected over the predicted location of the north wall of the Gulf Stream, during long transit passes between the buoy and the Gulf Stream box patterns. See Fig. 7. Data were collected at altitudes of both 5 kft and 17 kft.

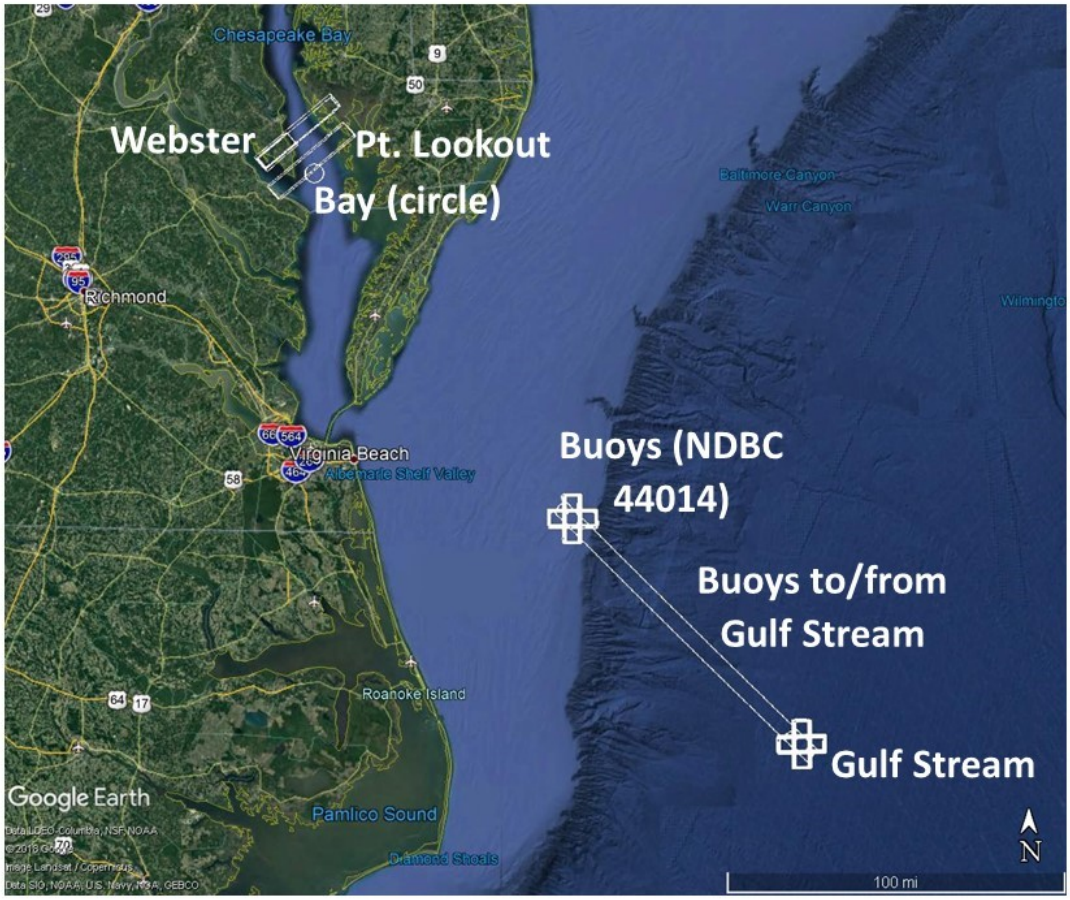

Fig. 7 Locations of the UINSAR passes flown on July 31, 2017

UINSAR Pass Summary

2017_07_31

Passes

Timestamp	Passname	Mode	Heading (deg)	SOG (m/s)
20170731_192113	17k buoys east	17k ping-pong short	90	149
20170731_193257	17k buoys west	17k ping-pong short	270	149
20170731_194043	17k buoys south	17k ping-pong short	180	123
20170731_194701	17k buoys north	17k ping-pong short	0	152
20170731_195259	17k buoys circle	17k clutter circular	180	
20170731_200850	5k buoys east	5k ping-pong short	90	121
20170731_201607	5k buoys west	5k ping-pong short	270	127
20170731_203006	5k buoys north	5k ping-pong short	0	124
20170731_203409	5k buoys south	5k ping-pong short	180	105
20170731_204009	5k buoys circle	5k clutter circular	0	105-152
20170731_205201	5k buoys to Gulf Stream	5k ping-pong long	135	125
20170731_211945	5k Gulf Stream circle	5k clutter circular	0	105-152
20170731_213227	5k Gulf Stream east	5k ping-pong short	90	117
20170731_214215	5k Gulf Stream west	5k ping-pong short	270	127

20170731_214914	5k Gulf Stream south	5k ping-pong short	180	128
20170731_215814	5k Gulf Stream north	5k ping-pong short	0	124
20170731_220857	17k GulfStream circle	17k clutter circular	180	105-152
20170731_222227	17k GulfStream east	17k ping-pong short	90	156
20170731_223025	17k GulfStream west	17k ping-pong short	270	147
20170731_223716	17k GulfStream south	17k ping-pong short	180	154
20170731_224439	17k GulfStream north	17k ping-pong short	0	143
20170731_225238	17k GulfStream to buoys	17k ping-pong long	315	144
20170731_230029	17k GulfStream to buoys	17k ping-pong long	315	122
20170731_235218	17k ping-pong linear - Pt Lookout 60	17k ping-pong linear	48.8	X
20170801_000314	17k ping-pong linear - Pt Lookout 240	17k ping-pong linear	228.8	X
20170801_001225	17k clutter circular - Bay	17k clutter circular	0	X
20170801_002635	17k ping-pong linear - Webster 240	17k ping-pong linear	228.8	X
20170801_003752	17k ping-pong linear - Webster 60	17k ping-pong linear	48.8	X
20170801_004525	5k ping-pong linear - Webster 240	5k ping-pong linear	228.8	X
20170801_010109	5k ping-pong linear - Webster 60	5k ping-pong linear	48.8	X

Table 4 Pass Summary for July 31, 2017

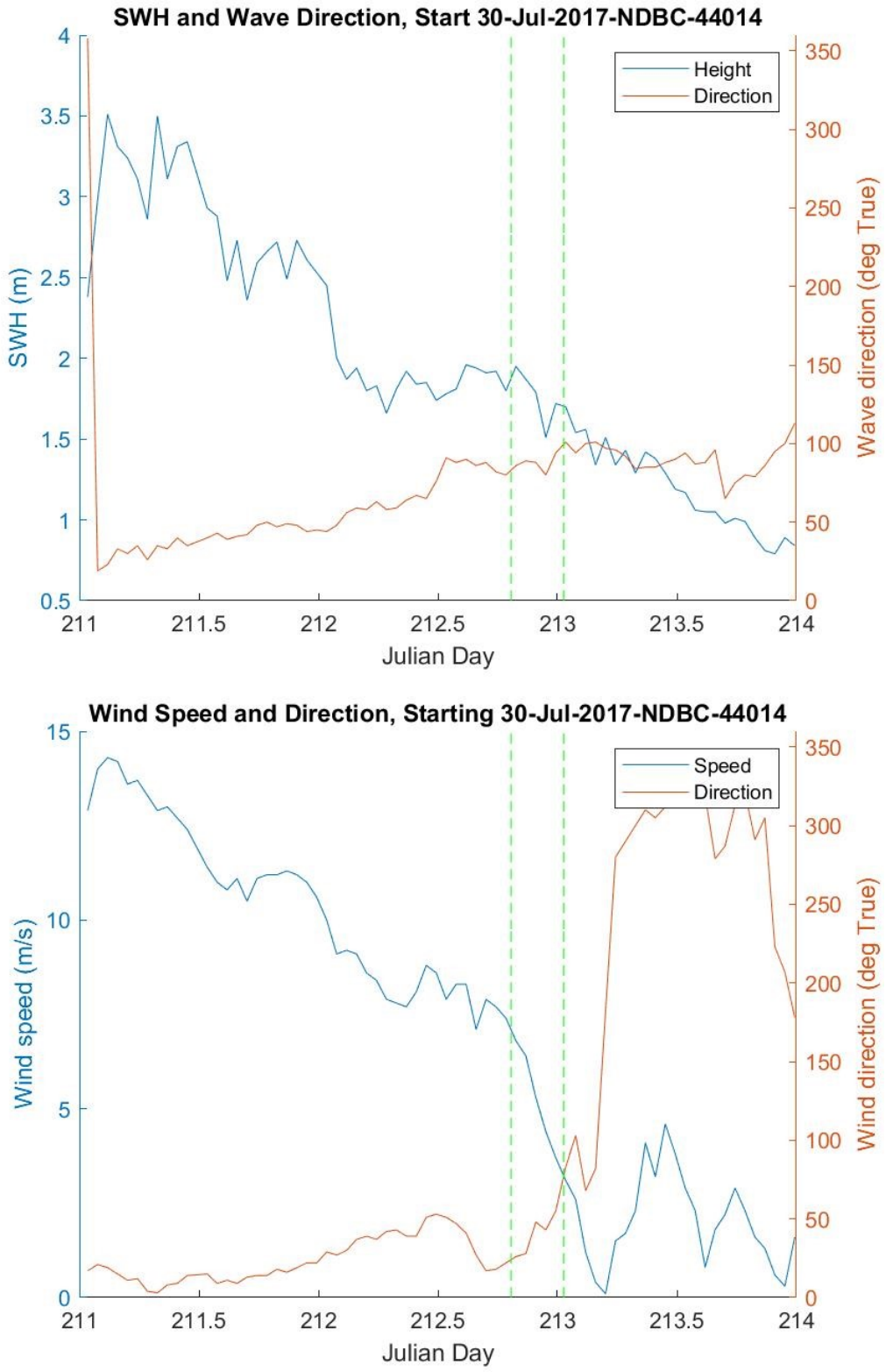

Fig. 8 (Upper) Significant wave height and dominant wave direction, and **(Lower)** wind speed and direction, as measured at NDBC 44014 around July 31 (Julian Day 212), 2017. The green vertical lines indicate the start and end of the UINSAR collection on that day.

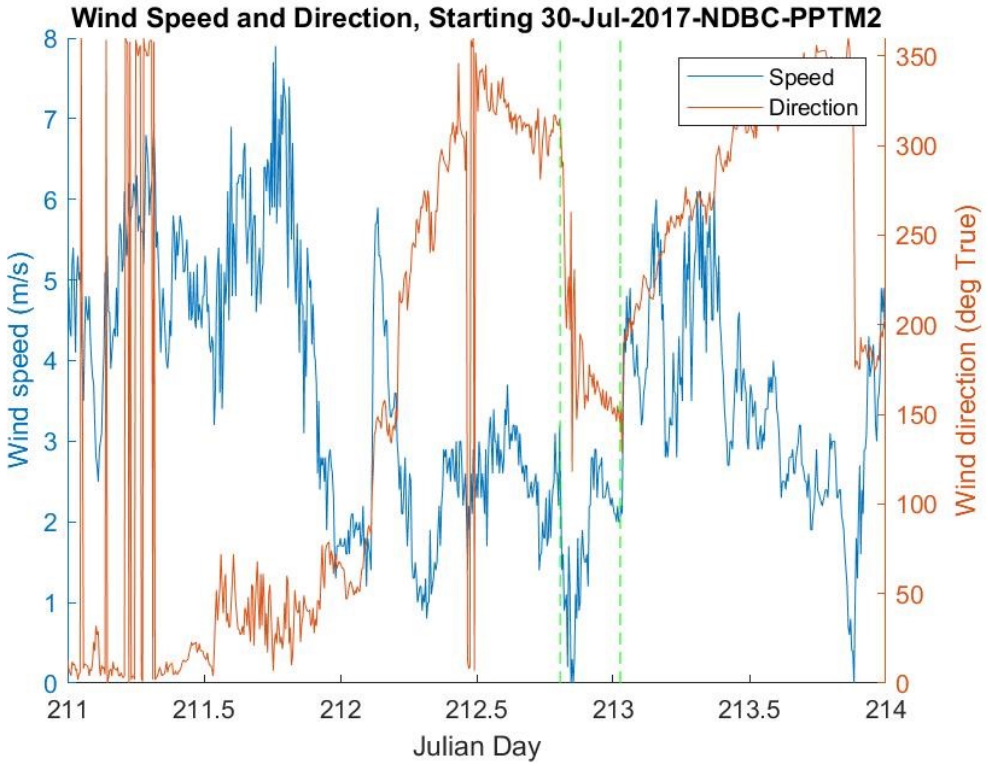

Fig. 9 Wind speed and direction, as measured at NDBC PPTM2 around July 31 (Julian Day 212), 2017. The green vertical lines indicate the start and end of the UINSAR collection on that day.

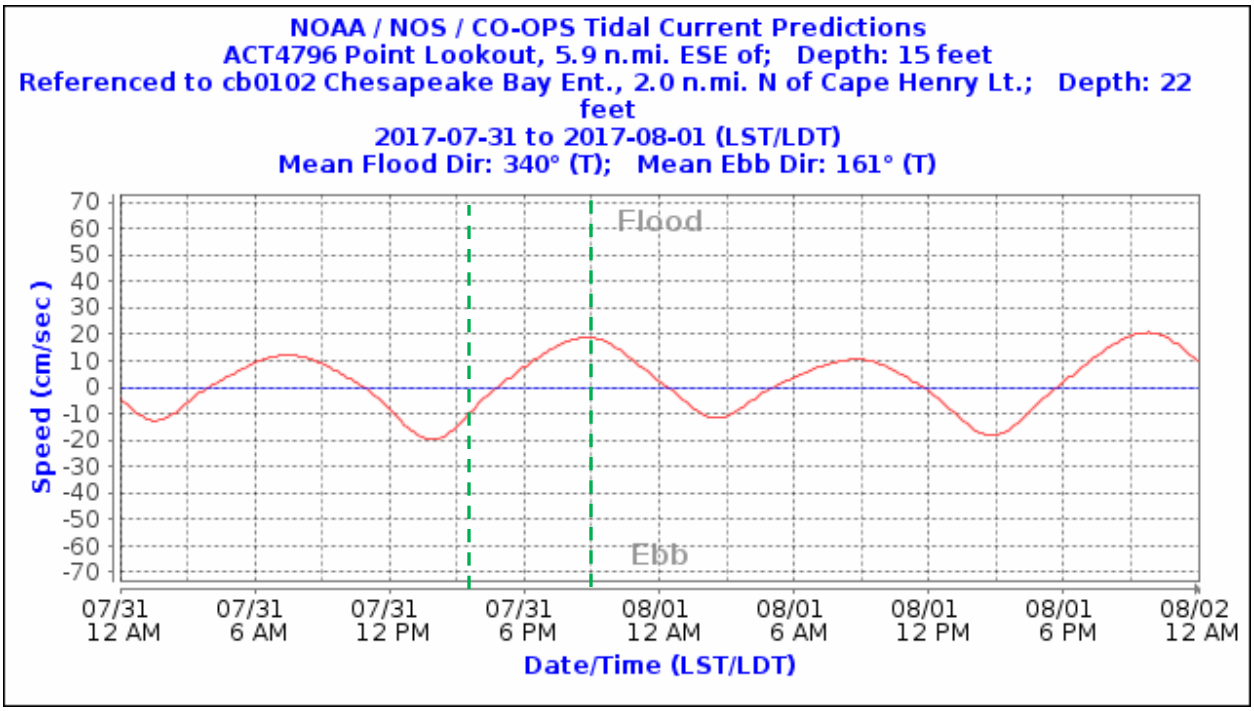

Fig. 10 Predicted tidal currents near Point Lookout (NOAA Station ACT4796) around July 31, 2017. Note that the time is given as Local Time. Add 4 hours to convert to UTC. The green vertical lines indicate the start and end of the UINSAR collection on that day.

5.2 January 18, 2018

On January 18, 2018, data were collected using linear passes over Webster Field and the anticipated position of the Gulf Stream east of the mouth of the Chesapeake Bay. Box patterns providing data with all cardinal look directions were also flown over NOAA NDBC 44009 east of the DE/MD border. See Fig. 11. All data were collected at a nominal altitude of 17 kft.

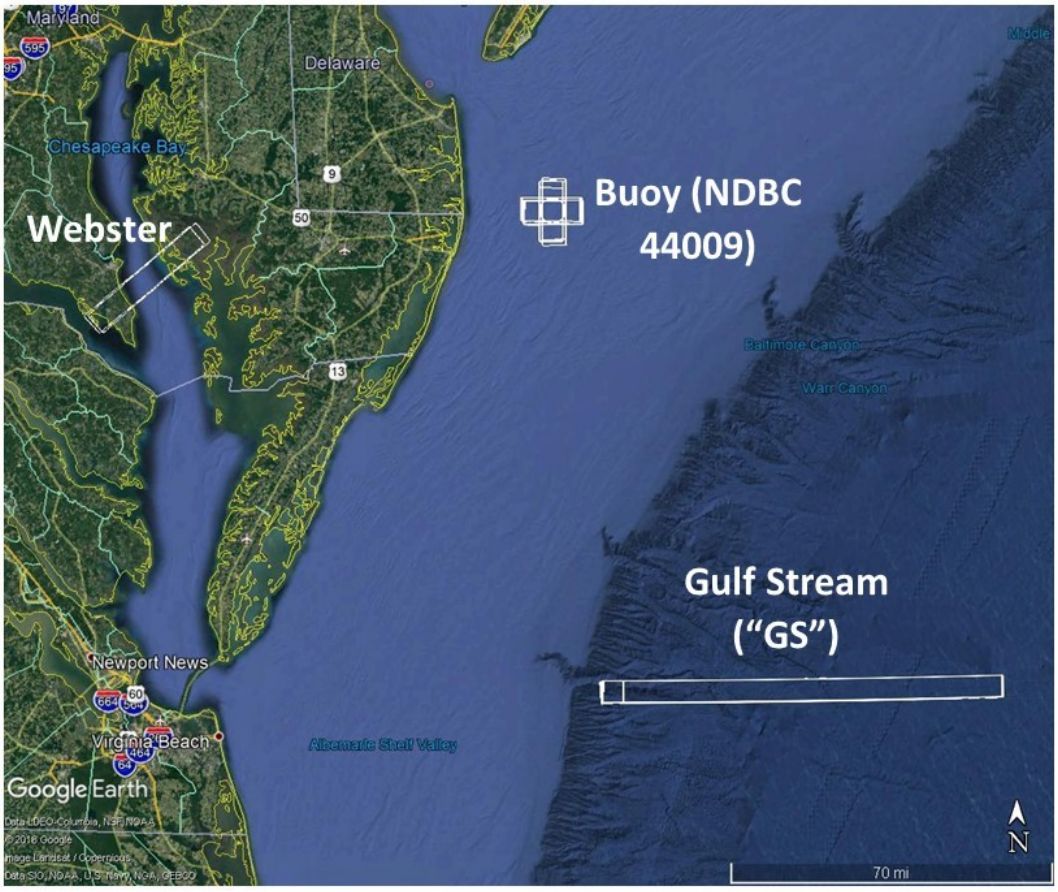

Fig. 11 Locations of the UINSAR passes flown on Jan 18, 2018

UINSAR Pass Summary

2018_01_18

Passes

Timestamp	Passname	Mode	Heading (deg)	SOG (m/s
20180118_203716	17k ping-pong Webster 240	17k ping-pong linear 40km	228.8	145
20180118_205326	17k ping-pong Webster 60	17k ping-pong linear 40km	48.8	119
20180118_210308	17k ping-pong Pt Lookout 240	17k ping-pong linear 40km Bad	228.8	X
20180118_212209	17k clutter GS E	17k clutter linear 130km	90	135
20180118_215118	17k ping-pong GS W	17k ping-pong linear 130km	270	117
20180118_222705	17k clutter Buoy N	17k clutter linear Bad	0	X
20180118_222842	17k clutter Buoy N	17k clutter linear	0	124
20180118_223646	17k ping-pong Buoy S	17k ping-pong linear	180	148
20180118_224317	17k ping-pong Buoy N	17k ping-pong linear	0	124
20180118_224922	17k clutter Buoy S	17k clutter linear	180	150
20180118_225511	17k clutter Buoy E	17k clutter linear	90	126
20180118_230138	17k clutter Buoy W	17k clutter linear- Bad	180	X
20180118_230253	17k clutter Buoy W	17k clutter linear	270	114
20180118_230815	17k clutter Buoy Circle S	17k clutter circular	180	114-150

20180118_232017	17k ping-pong Buoy Circle S	17k ping-pong circular	180	114-150
20180118_232653	17k ping-pong Buoy E	17k ping-pong linear	90	133
20180118_233348	17k ping-pong Buoy W	17k clutter linear	270	132
20180118_234200	17k clutter GS E	17k clutter linear 130km-Bad	90	X
20180118_235553	17k clutter GS E	17k clutter linear 130km	90	129
20180119_001525	17k ping-pong GS W	17k ping-pong linear 130km	270	126

Table 5 Pass Summary for Jan 18, 2018

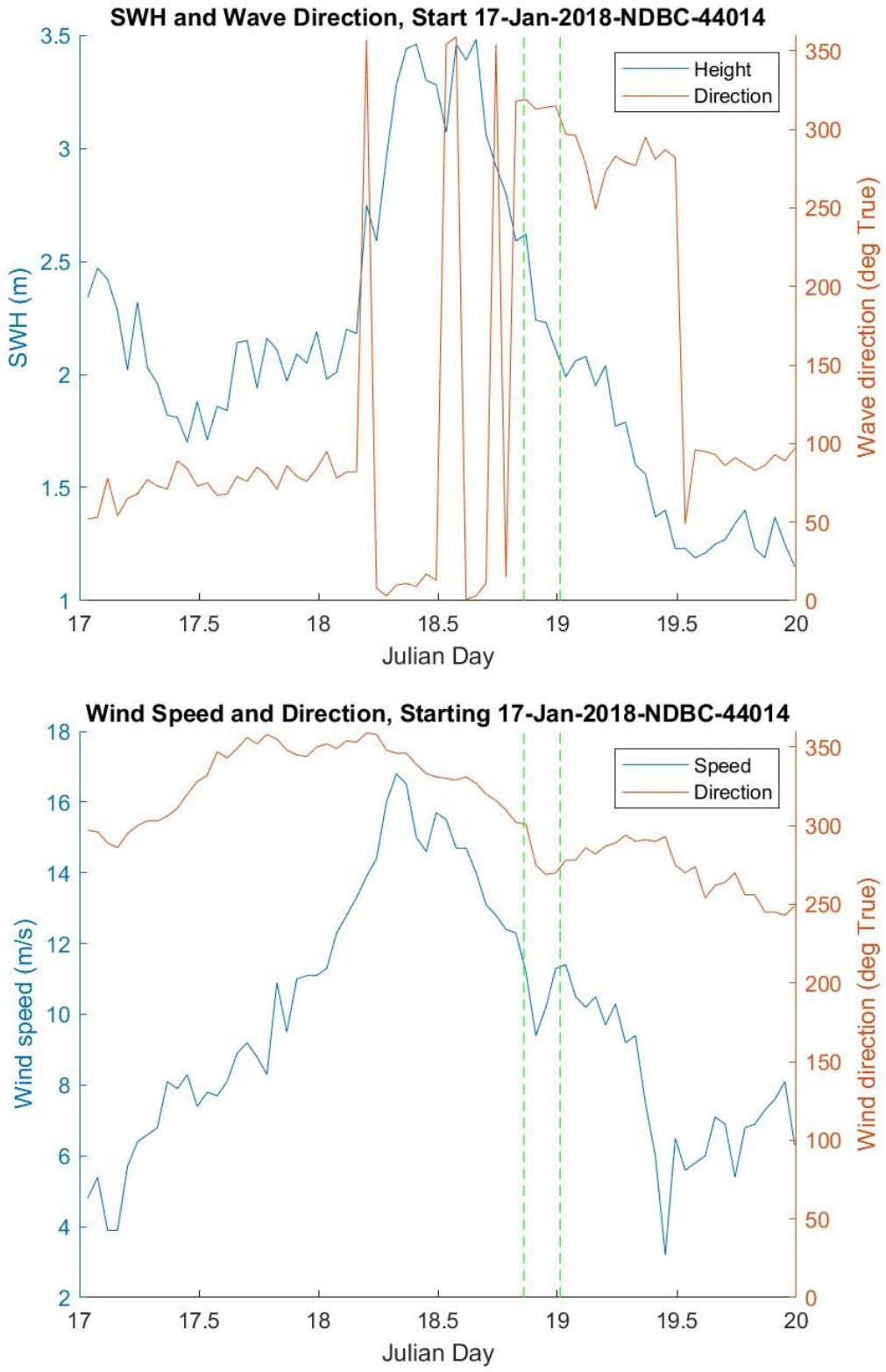

Fig. 12 (Upper) Significant wave height and dominant wave direction, and **(Lower)** wind speed and direction, as measured at NDBC 44014 around Jan 18 (Julian Day 18), 2018. The green vertical lines indicate the start and end of the UINSAR collection on that day.

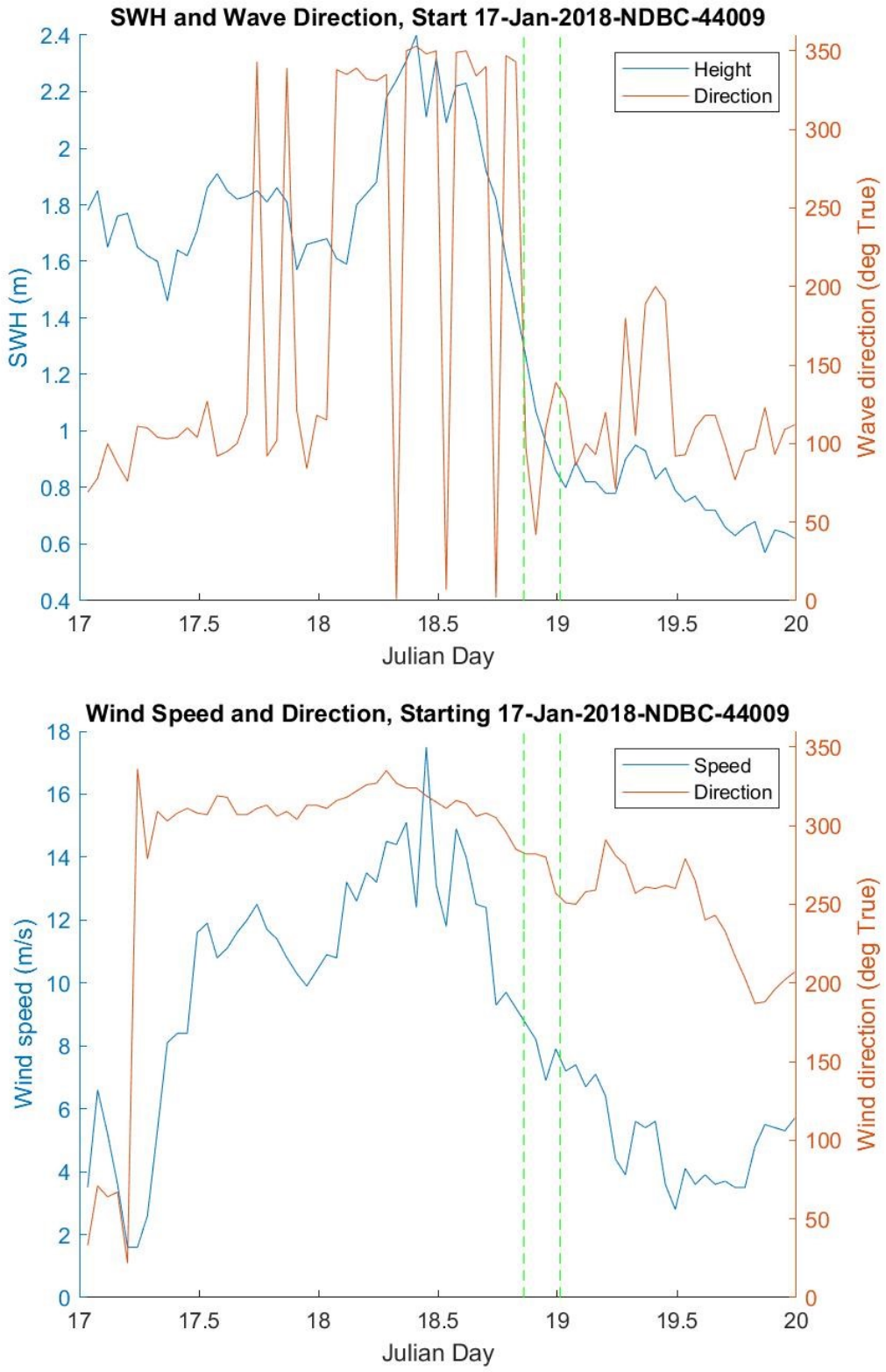

Fig. 13 (Upper) Significant wave height and dominant wave direction, and **(Lower)** wind speed and direction, as measured at NDBC 44009 around Jan 18 (Julian Day 18), 2018. The green vertical lines indicate the start and end of the UINSAR collection on that day.

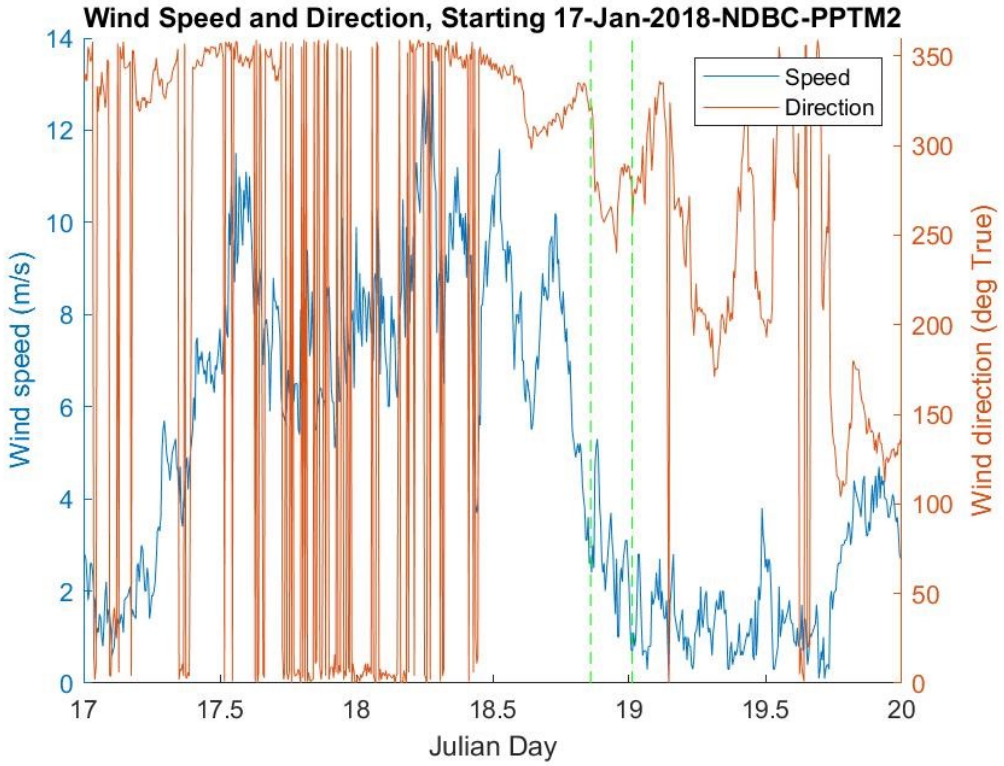

Fig. 14 Wind speed and direction, as measured at NDBC PPTM2 around Jan 18 (Julian Day 18), 2018. The green vertical lines indicate the start and end of the UINSAR collection on that day.

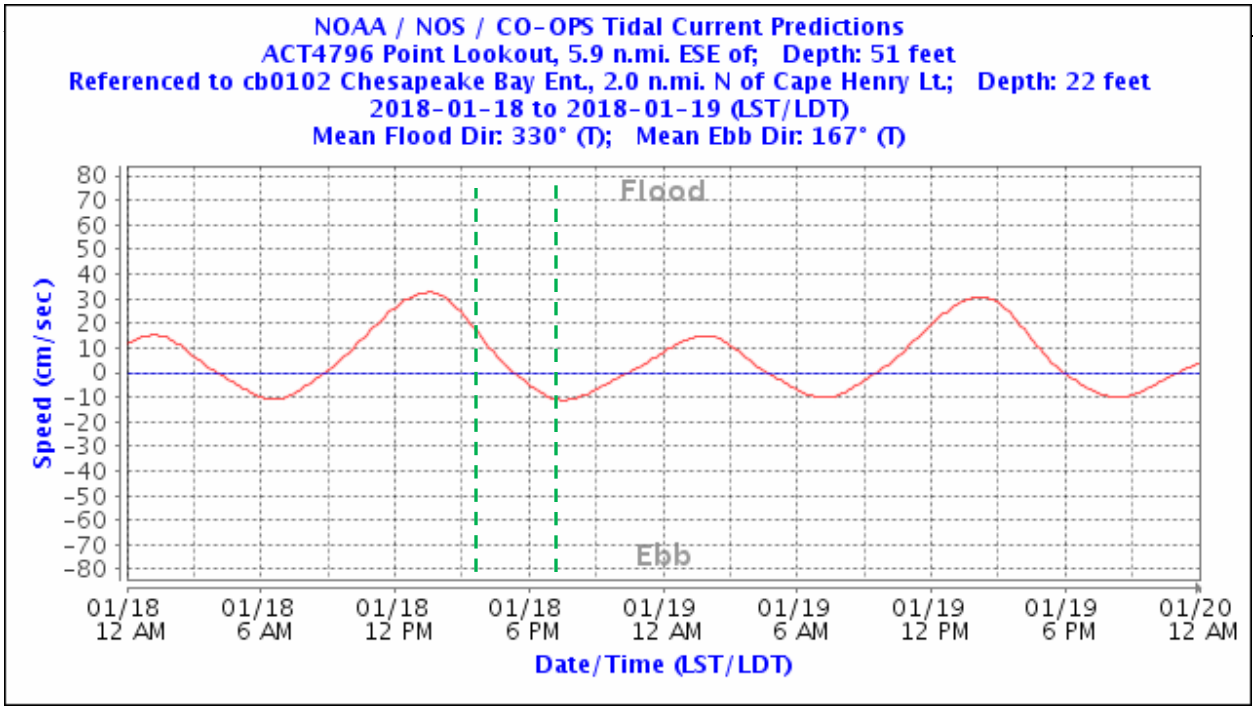

Fig. 15 Predicted tidal currents near Point Lookout (NOAA Station ACT4796) around Jan 18, 2018. Note that the time is given as Local Time. Add 5 hours to convert to UTC. The green vertical lines indicate the start and end of the UINSAR collection on that day.

5.3 January 23, 2018

On January 23 2018, data were collected over Webster Field using linear passes, over NOAA NDBC buoy 44014 using box patterns, over the Gulf Stream using a circle pattern, and along a transit between the Gulf Stream circle and the buoy. See Fig. 16. All data were collected at an altitude of 17 kft.

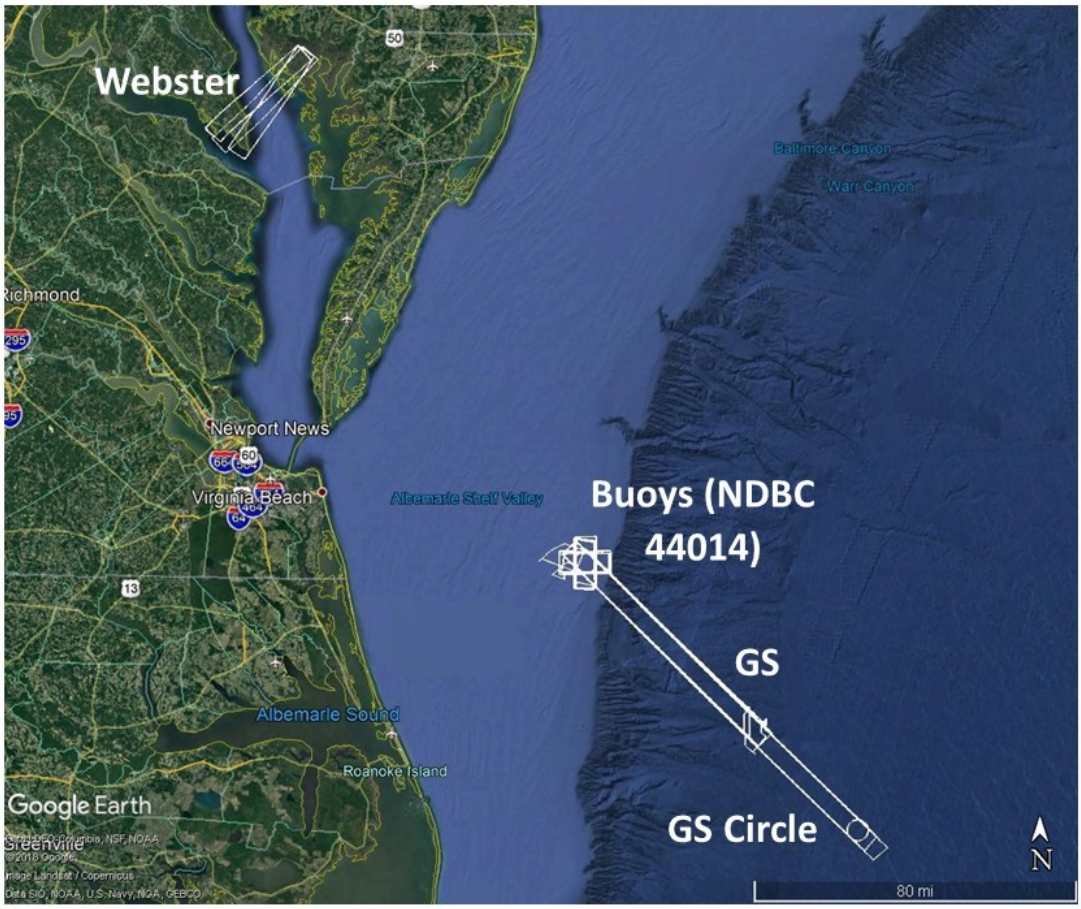

Fig. 16 Locations of the UINSAR passes flown on Jan 23, 2018

UINSAR Pass Summary

2018_01_23

Passes

Timestamp	Passname	Mode	Heading (deg)	SOG (m/s)
20180123_224355	17k GS clutter SE	17k clutter linear 130km Bad Track	135	X
20180123_225916	17k GS clutter SE	17k clutter linear 130km	135	131
20180123_231638	17k GS ping-pong NW	17k ping-pong linear 130km	315	127
20180123_233101	17k Buoy clutter circle SE	17k clutter circular	135	101-165
20180123_234214	17k Buoy ping-pong circle NW	17k ping-pong circular	315	101-165
20180123_234657	17k Buoy clutter S	17k clutter linear	180	101-165
20180123_235308	17k Buoy clutter N	17k clutter linear	0	151
20180123_235808	17k Buoy ping-pong S	17k ping-pong linear	180	107
20180124_000518	17k Buoy ping-pong N	17k ping-pong linear	0	151
20180124_000901	17k Buoy clutter W	17k clutter linear	270	101
20180124_001736	17k Buoy clutter E	17k clutter linear	90	163

20180124_002420	17k Buoy ping-pong W	17k ping-pong linear	270	102
20180124_003131	17k Buoy ping-pong E	17k ping-pong linear	90	165
20180124_004027	17k GS ping-pong SE	17k ping-pong linear 130km	135	139
20180124_010523	17k GS clutter circle NW	17k clutter circular	315	100-154
20180124_011606	17k GS ping-pong circle SE	17k ping-pong circular	135	100-154
20180124_012623	17k GS clutter NW	17k clutter linear 130km	315	129
20180124_021147	17k clutter Webster 60	17k clutter linear 40km	48.8	144
20180124_022730	17k clutter Webster 240	17k clutter linear 40km	228.8	129
20180124_023618	17k ping-pong Webster 60	17k ping-pong linear 40km	48.8	143
20180124_024530	17k ping-pong Webster 240	17k ping-pong linear 40km	228.8	132

Table 6 Pass Summary for Jan 23, 2018

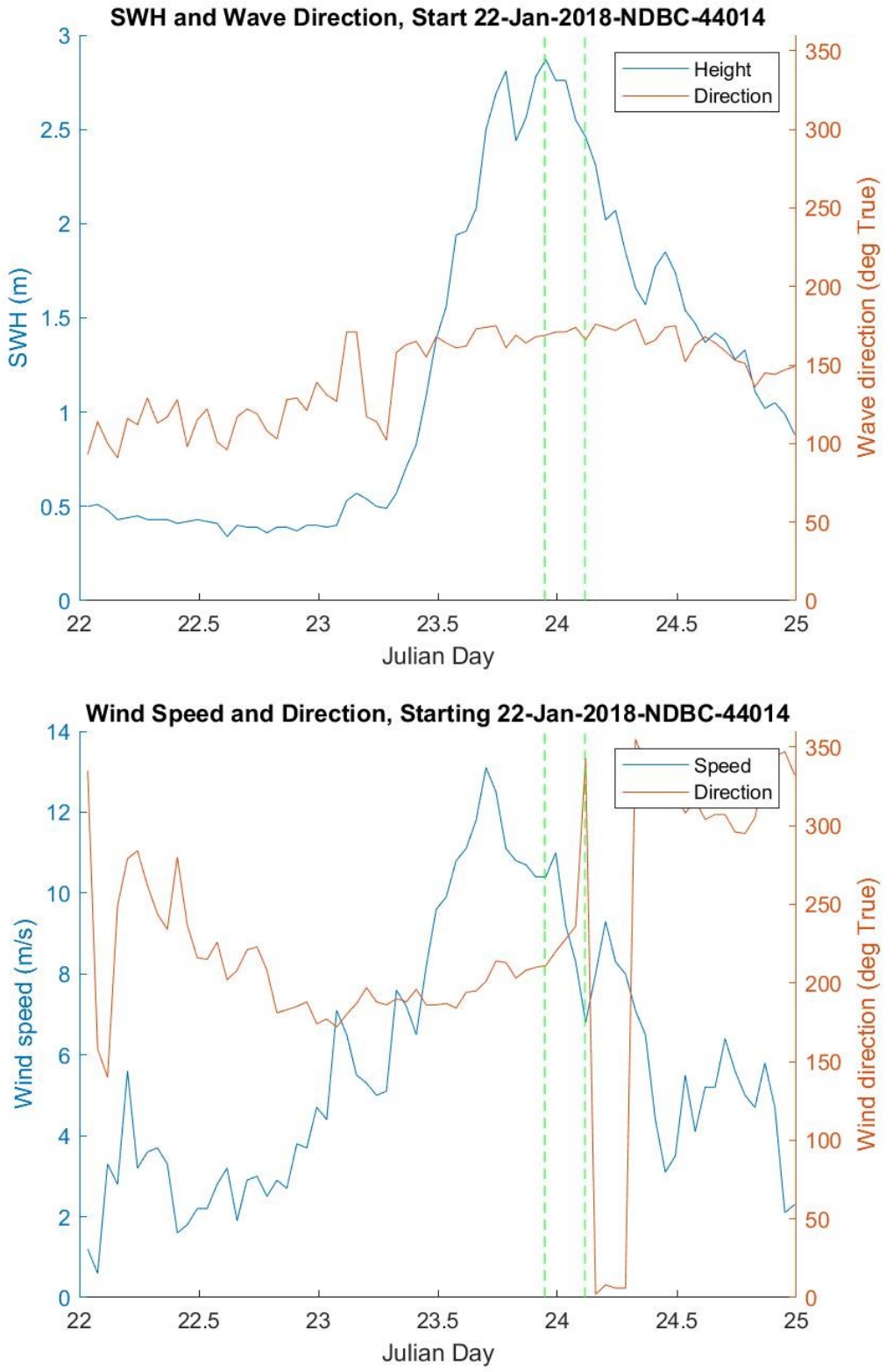

Fig. 17 (Upper) Significant wave height and dominant wave direction, and **(Lower)** wind speed and direction, as measured at NDBC 44014 around Jan 23 (Julian Day 23), 2018. The green vertical lines indicate the start and end of the UINSAR collection on that day.

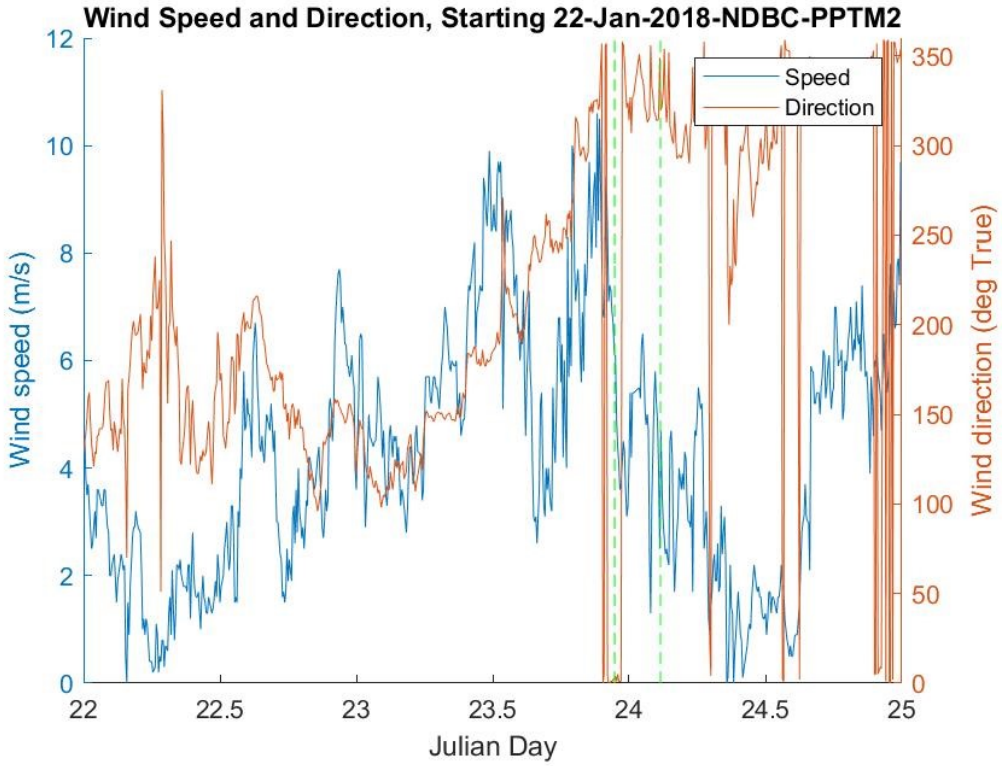

Fig. 18 Wind speed and direction, as measured at NDBC PPTM2 around Jan 23 (Julian Day 23), 2018. The green vertical lines indicate the start and end of the UINSAR collection on that day.

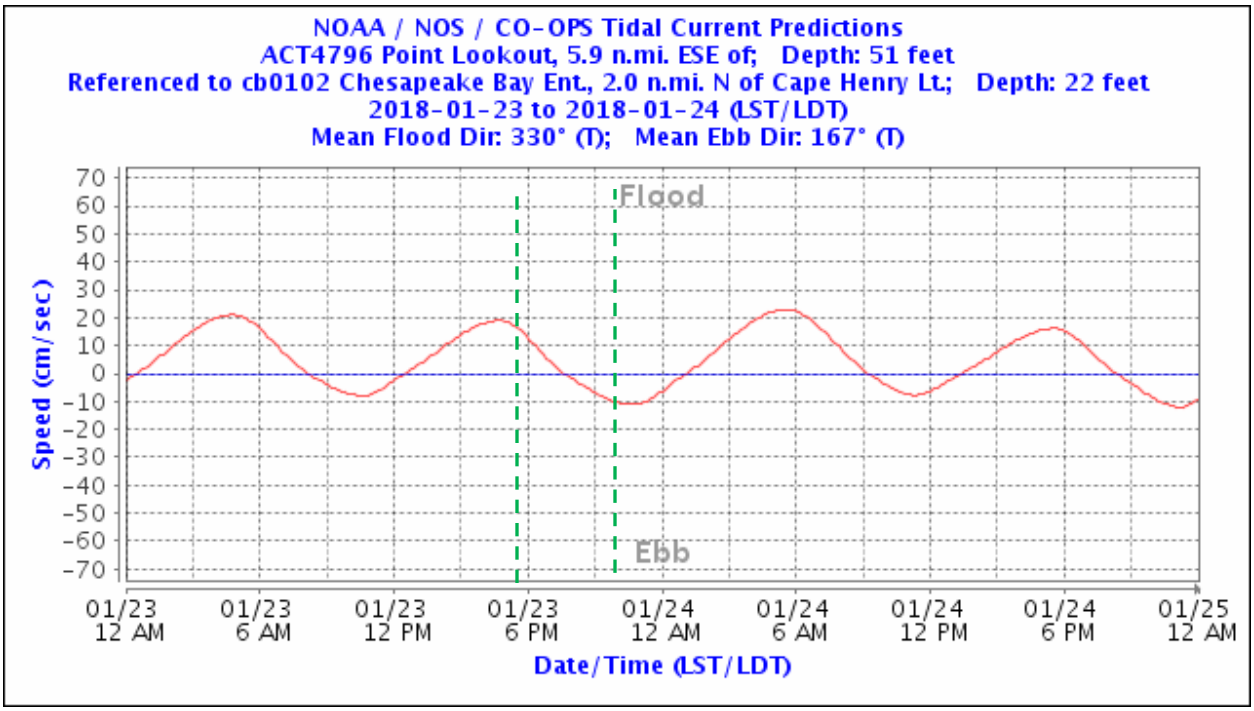

Fig. 19 Predicted tidal currents near Point Lookout (NOAA Station ACT4796) around Jan 23, 2018. Note that the time is given as Local Time. Add 5 hours to convert to UTC. The green vertical lines indicate the start and end of the UINSAR collection on that day. (22:45=17:45=5:45, 02:45=21:45=9:45)

5.4 January 30, 2018

On January 30 2018, data were collected over Webster Field using linear passes, over NOAA NDBC buoy 44014 using box patterns, over the Gulf Stream using a circle pattern, and along a transit between the Gulf Stream circle and the buoy. See Fig. 20. All data were collected at an altitude of 17 kft. As shown in Fig. 21, the highest wind speed (14 m/s) and significant wave height (3.5 m) of all the UINSAR flights occurred on this day.

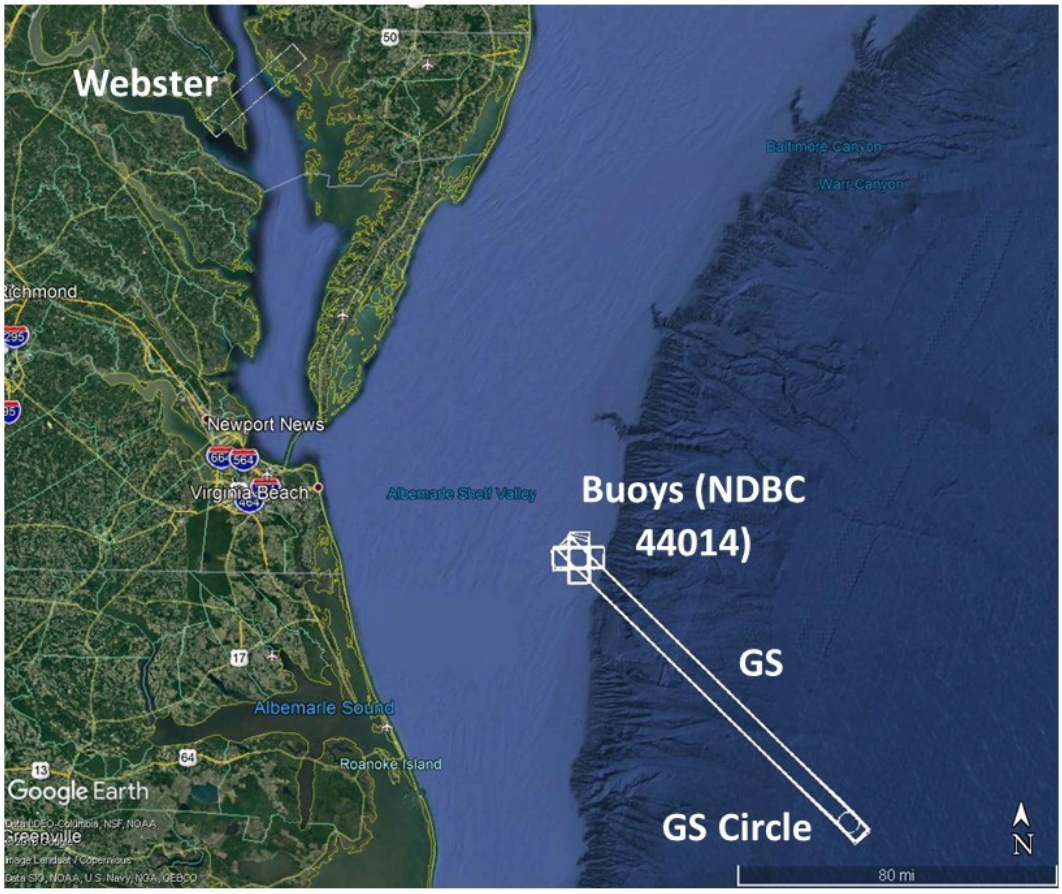

Fig. 20 Locations of the UINSAR passes flown on Jan 30, 2018

UINSAR Pass Summary

2018_01_30

Passes

Timestamp	Passname	Mode	Heading (deg)	SOG (m/s)
20180130_214514	17k clutter Webster 240	17k clutter linear 40km	228.8	147
20180130_221949	17k GS clutter SE	17k clutter linear 130km	135	129-162
20180130_224544	17k GS clutter circle NW	17k clutter circular	315	132-166
20180130_225459	17k GS ping-pong circle SE	17k ping-pong circular	135	132-166
20180130_230445	17k GS ping-pong NW	17k ping-pong linear 130km	315	131
20180130_232751	17k GS ping-pong SE	17k ping-pong linear 130km	135	168
20180130_234711	17k GS clutter NW	17k clutter linear 130km	315	111
20180131_001104	17k Buoy clutter circle SE	17k clutter circular	135	113-190
20180131_001825	17k Buoy ping-pong circle NW	17k ping-pong circular	315	113-190
20180131_002735	17k Buoy clutter S	17k clutter linear	180	164
20180131_003102	17k Buoy clutter N	17k clutter linear	0	116

20180131_003742	17k Buoy ping-pong S	17k ping-pong linear	180	175
20180131_004302	17k Buoy ping-pong N	17k ping-pong linear	0	118
20180131_004927	17k Buoy clutter W	17k clutter linear	270	
20180131_005033	17k Buoy clutter W	17k clutter linear	270	118
20180131_005723	17k Buoy clutter E	17k clutter linear	90	171
20180131_010201	17k Buoy ping-pong W	17k ping-pong linear	270	111
20180131_010955	17k Buoy ping-pong E	17k ping-pong linear	90	165

Table 7 Pass Summary for Jan 30, 2018

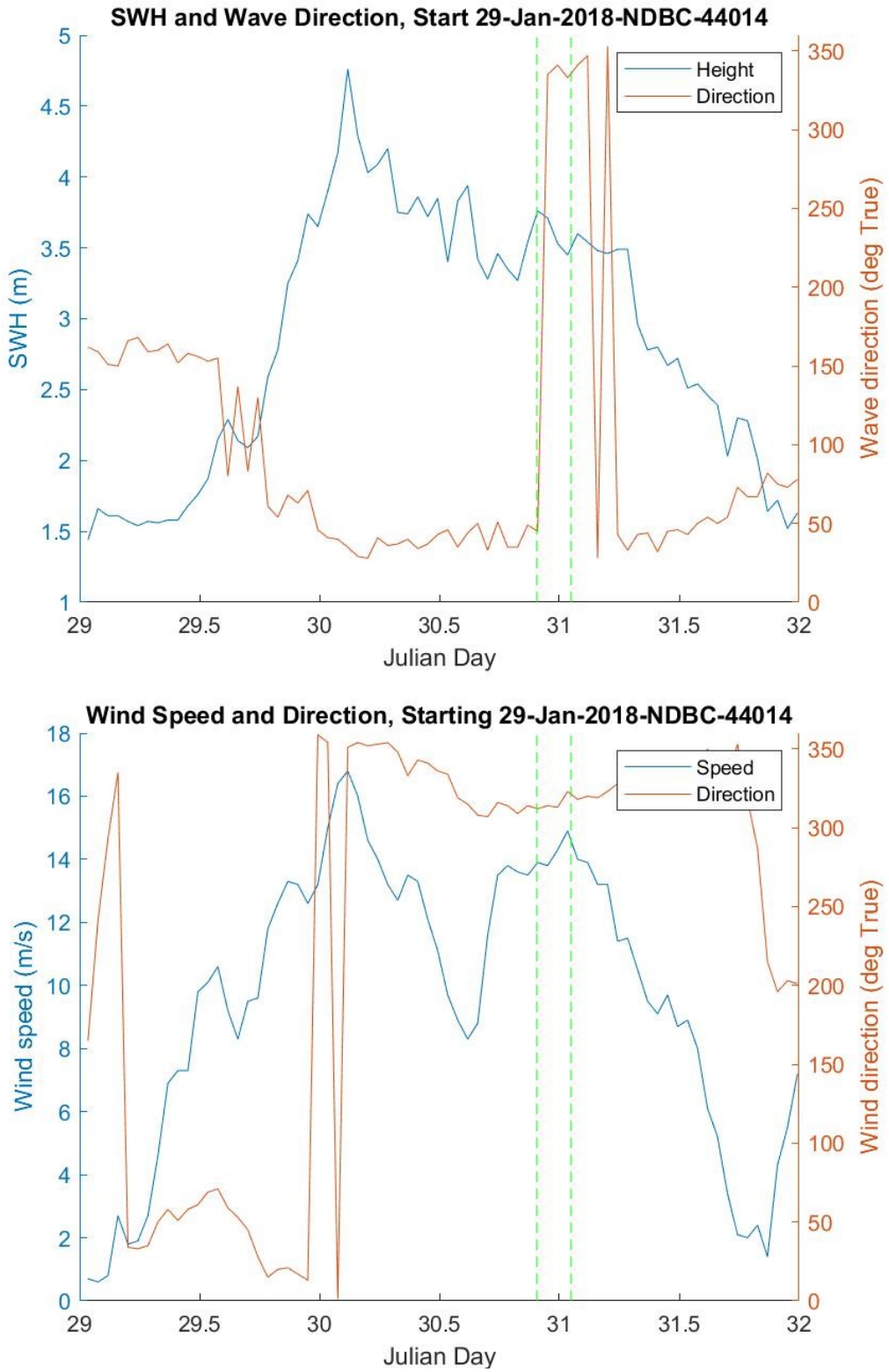

Fig. 21 (Upper) Significant wave height and dominant wave direction, and **(Lower)** wind speed and direction, as measured at NDBC 44014 around Jan 30 (Julian Day 30), 2018. The green vertical lines indicate the start and end of the UINSAR collection on that day.

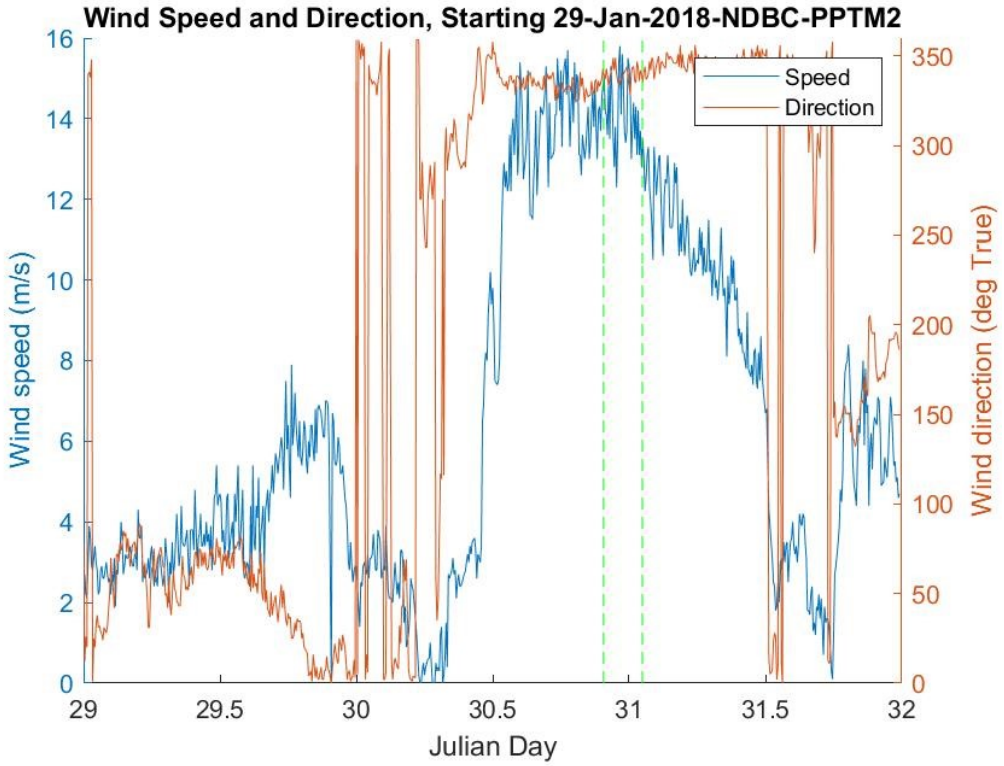

Fig. 22 Wind speed and direction, as measured at NDBC PPTM2 around Jan 30 (Julian Day 30), 2018. The green vertical lines indicate the start and end of the UINSAR collection on that day.

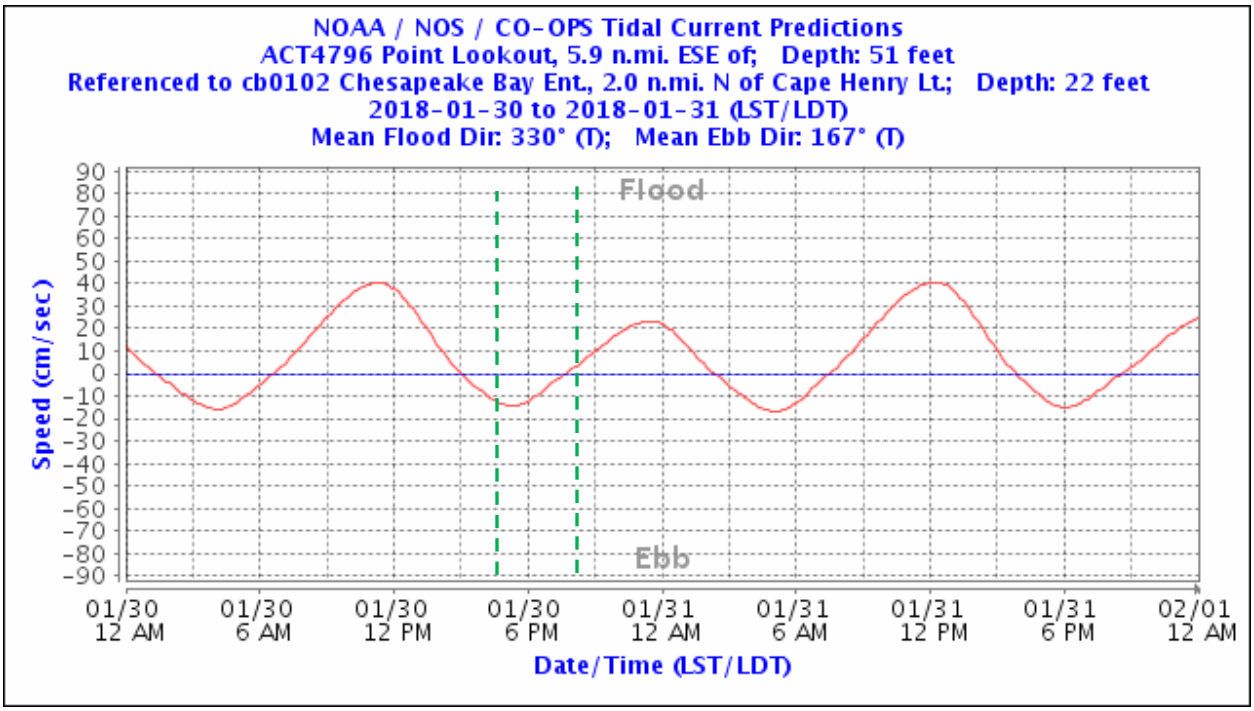

Fig. 23 Predicted tidal currents near Point Lookout (NOAA Station ACT4796) around Jan 30, 2018. Note that the time is given as Local Time. Add 5 hours to convert to UTC. The green vertical lines indicate the start and end of the UINSAR collection on that day. (21:45=16:45=4:45, 01:10=20:10=8:10)

5.5 February 5, 2018

On February 5, 2018, areas around Webster Field and Pt. Lookout were imaged using both linear and circle passes. See Fig. 24. All passes were flown at an altitude of 5 kft. As shown in Fig. 26, the highest predicted tidal currents of all the UINSAR flights occurred on this day.

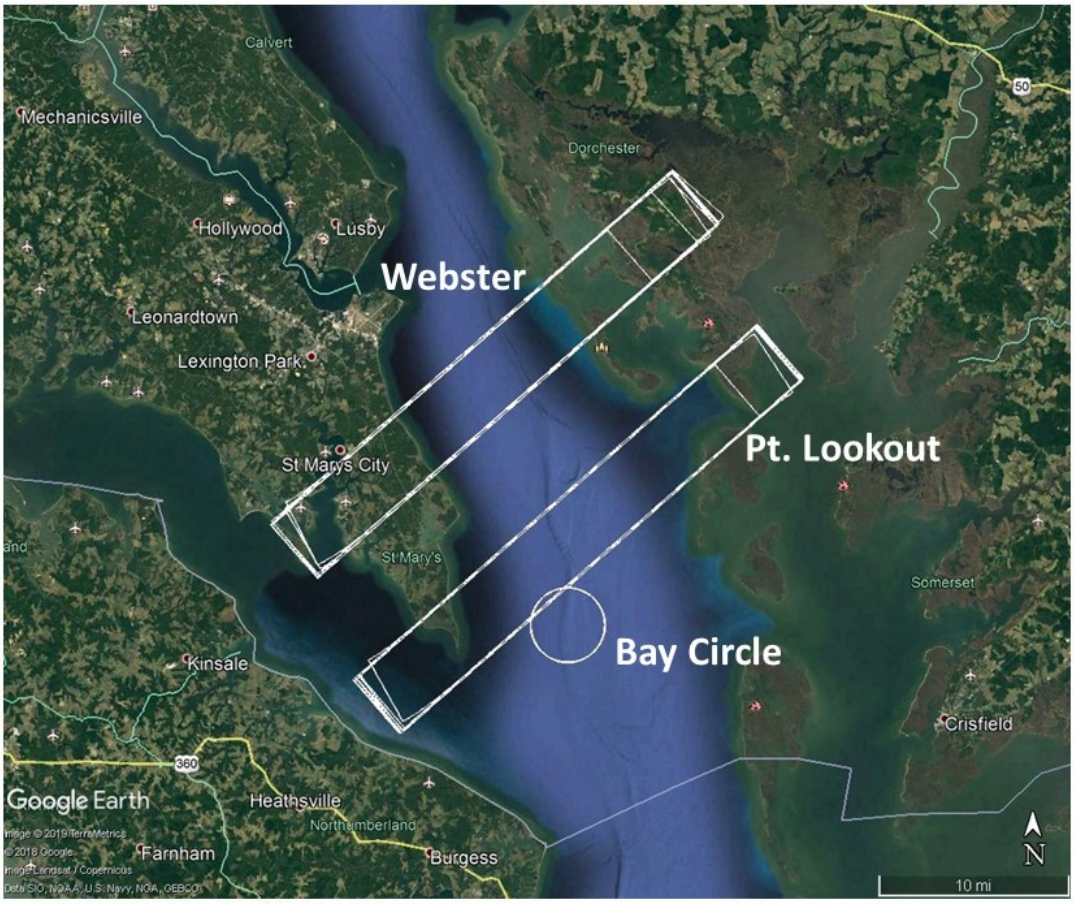

Fig. 24 Locations of the UINSAR passes flown on Feb 5, 2018

UINSAR Pass Summary

2018_02_05

Passes

Timestamp	Passname	Mode	Heading (deg)	SOG (m/s)
20180205_201828	5k clutter Webster 240	5k clutter linear 40km	228.8	129
20180205_202130	5k clutter Webster 240	5k clutter linear 40km	228.8	130
20180205_202639	5k clutter Webster 60	5k clutter linear 40km	48.9	127
20180205_203520	5k ping-pong Webster 240	5k ping-pong linear 40km	228.8	127
20180205_204449	5k ping-pong Webster 60	5k ping-pong linear 40km	48.9	126
20180205_205401	5k clutter Pt Lookout 240	5k clutter linear 40km	228.8	126
20180205_210424	5k clutter Pt Lookout 60	5k clutter linear 40km	48.8	129
20180205_211403	5k ping-pong Pt Lookout 240	5k ping-pong linear 40km	228.8	124
20180205_212234	5k ping-pong Pt Lookout 60	5k ping-pong linear 40km	48.8	135
20180205_213133	5k clutter circle Bay 240	5k clutter circular- Bad	228.9	X
20180205_213413	5k clutter circle Bay 240	5k clutter circular	228.9	122-125
20180205_214141	5k ping-pong circle Bayt 60	5k ping-pong circular	54.9	122-125

20180205_215133	5k clutter Webster 240	5k clutter linear 40km	228.8	119
20180205_220319	5k clutter Webster 60	5k clutter linear 40km	48.9	130
20180205_221139	5k ping-pong Webster 240	5k ping-pong linear 40km	228.8	120
20180205_222142	5k ping-pong Webster 60	5k ping-pong linear 40km	48.9	129
20180205_222928	5k clutter Pt Lookout 240	5k clutter linear 40km	228.8	121
20180205_223955	5k clutter Pt Lookout 60	5k clutter linear 40km	48.8	131
20180205_224834	5k ping-pong Pt Lookout 240	5k ping-pong linear 40km - Bad	228.8	X
20180205_224904	5k ping-pong Pt Lookout 240	5k ping-pong linear 40km	228.8	121
20180205_225755	5k ping-pong Pt Lookout 60	5k ping-pong linear 40km	48.8	132
20180205_230944	5k clutter circle Bay 240	5k clutter circular	228.9	122-132
20180205_231634	5k ping-pong circle Bayt 60	5k ping-pong circular	54.9	122-132
20180205_232731	5k ping-pong Pt Lookout 60	5k ping-pong linear 40km	48.8	131

Table 8 Pass Summary for Feb 5, 2018

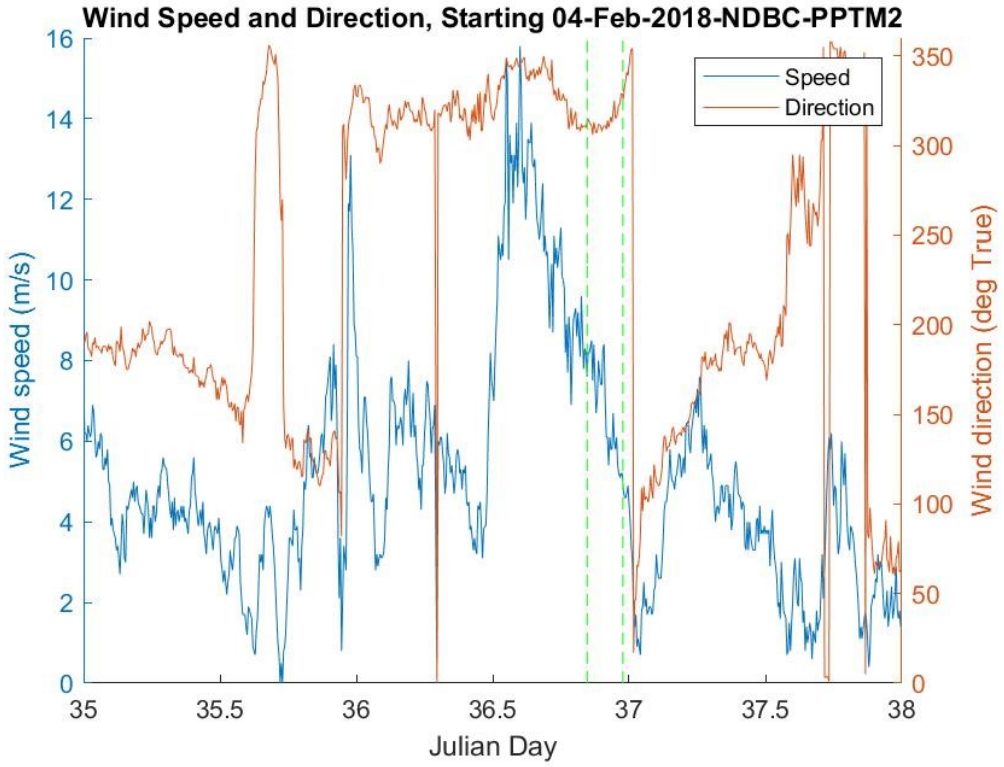

Fig. 25 Wind speed and direction, as measured at NDBC PPTM2 around Feb 5 (Julian Day 36), 2018. The green vertical lines indicate the start and end of the UINSAR collection on that day.

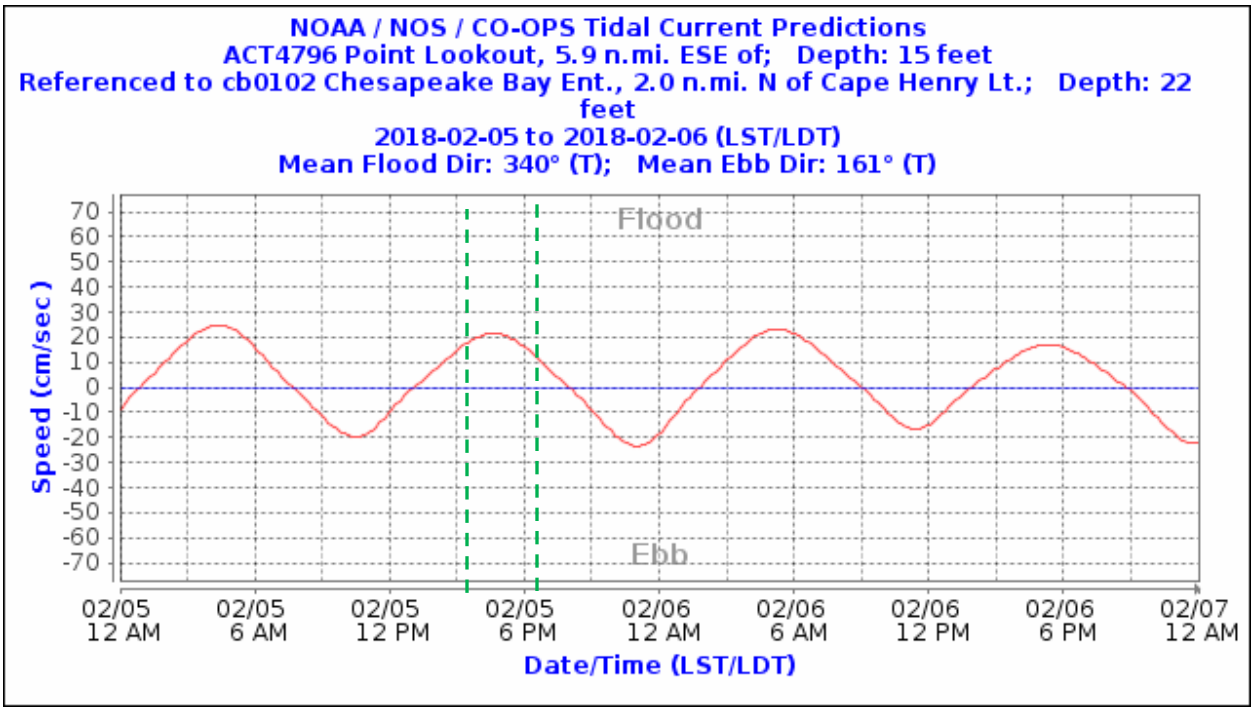

Fig. 26 Predicted tidal currents near Point Lookout (NOAA Station ACT4796) around Feb 5, 2018. Note that the time is given as Local Time. Add 5 hours to convert to UTC. The green vertical lines indicate the start and end of the UINSAR collection on that day. (20:18=15:18=3:18, 23:27=18:27=6:27)

6. Calibration Target

A large metal "tophat" reflector was present in an open area of Webster Field during the deployment. See Fig. 27. This target provides a strong UHF point response for any look direction, and was located at approximately 38.13425° N, 76.43584° W. The UINSAR imagery of the generally flat (and stationary) terrain in and around Webster Field can also serve as an ATI phase reference.

Fig. 27 a) Photograph of the metal tophat reflector present at Webster Field during the deployments. The height of the central cylinder is approximately 1 m.

Fig. 27 b) Approximate location of the tophat at Webster Field. This area is located in the southwest corner of the facility.

REFERENCES

[1] Goldstein, R. M., and H. A. Zebker, "Interferometric radar measurement of ocean surface currents", *Nature*, Vol 328, August 1987

[2] Toporkov, J. et al, "Sea Surface Velocity Vector Retrieval Using Dual-Beam Interferometry: First Demonstration", *IEEE Trans on Geosci Remote Sensing*, Vol. 43, No. 11, November 2005

[3] Romeiser, R. et al, "First Analysis of TerraSAR-X Along-Track InSAR-Derived Current Fields", *IEEE Transactions on Geoscience and Remote Sensing*, Vol. 48, No. 2, February 2010

[4] Frasier, S and R. McIntosh, "Observed wavenumber-frequency properties of microwave backscatter from the ocean surface at near-grazing angles", J. Geophysical Research, Vol. 101, No. C8, Aug. 1996

[5] Dugan, J. et al, "Near-Surface Current Profile Measurements Using Time Series Optical Imagery", *Proceedings of the IEEE/OES/CMTC Ninth Working Conference on Current Measurement Technology*, Charlston SC, USA, March 2008